Historical and projected forest cover changes in the Mount Kenya Ecosystem: Implications for sustainable forest management

Brian Rotich [a,b,*] , Abdalrahman Ahmed [c,d], Benjamin Kinyili [e], Harison Kipkulei [f,g,h]

[a] Institute of Environmental Sciences, Hungarian University of Agriculture and Life Sciences, Gödöllő, H-2100, Hungary
[b] Faculty of Environmental Studies and Resources Development, Chuka University, P.O. Box 109-60400, Chuka, Kenya
[c] Institute of Geomatics and Civil Engineering, Faculty of Forestry, University of Sopron. Bajcsy-Zs 4, Sopron, 9400, Hungary
[d] Department of Forest and Environment, Faculty of Forest Science and Technology, University of Gezira, Sudan
[e] Kenya Forest Service, Department of Forest Survey and Information Management, P.O Box 30513-00100, Nairobi, Kenya
[f] Department of Geomatic Engineering and Geospatial Information Systems, Jomo Kenyatta University of Agriculture and Technology, P.O. Box, 62000 00200, Nairobi, Kenya
[g] Leibniz Centre for Agricultural Landscape Research (ZALF) Eberswalder Straße 84, 15374, Müncheberg, Germany
[h] University of Augsburg, Faculty of Applied Computer Sciences, Institute of Geography, Alter Postweg 118, 86159, Augsburg, Germany

ARTICLE INFO

ABSTRACT

Understanding historical patterns of forest cover change (FCC) is critical for predicting future trends and informing sustainable management strategies. This study quantified and analyzed historical and projected FCC in the Mount Kenya Ecosystem (MKE), central Kenya. Land Use Land Cover (LULC) maps for 2000, 2014, and 2023 were classified using Random Forest (RF) in Google Earth Engine (GEE). Explanatory factors of LULC change (slope, aspect, population density, proximity to rivers, roads, and towns) were used to project LULC for 2035 using Cellular Automata and Markov Chain Analysis (CA-MCA).

Six LULC types (open forest, closed forest, cropland, bareland, built-up, shrubland and grassland) were successfully classified with accuracies exceeding 82.5% and Kappa coefficients above 0.77. Between 2000 and 2023, open forest ($+201.12$ km^2), cropland ($+218$ km^2), bareland ($+290.09$ km^2), and built-up areas ($+0.27$ km^2) expanded, while closed forest (-141.55 km^2) and shrubland and grassland (-567.93 km^2) declined. An overall Kappa coefficient value of 0.78 and an accuracy of 82% indicated good results for LULC statistics and projected map for 2035. LULC projections for the year 2035 under the Business as Usual (BAU) scenario suggest continued expansion of cropland ($+174.70$ km^2), built-up areas ($+0.49$ km^2), and open forest ($+471.72$ km^2), with declines in closed forest (-423.53 km^2) and shrubland and grassland (-357.79 km^2).

These results highlight the ongoing pressures on the MKE's biodiversity and ecosystem services. The study's methods offer a replicable framework for assessing FCC in similar ecosystems to inform evidence-based conservation and land management policies.

1. Introduction

Forests are significant self-regulating natural resources that offer a broad range of terrestrial functions in addition to providing multiple ecosystem goods and services to human society (Krieger, 2001; Mishkin and Pacheco, 2022; Simeon and Wana, 2024). Forest Cover Change (FCC) affects the delivery of important ecosystem services, including climate regulation, biodiversity richness, water supplies, and carbon sequestration (Balthazar et al., 2015; Foley et al., 2005). Changes in forest cover are driven by multifaceted processes that are dependent on

biophysical, political, social, economic, and conservation conditions (Vanonckelen and Van Rompaey, 2015). Globally, different patterns of losses and gains in forest cover have been documented (FAO, 2015; Guo et al., 2022; Margono et al., 2014; Paradis, 2021; Rotich and Ojwang, 2021; Saranya et al., 2022; Tesfay et al., 2023; Yahya et al., 2020). Forest cover gains are mainly driven by favorable afforestation policies, intensive forestry, natural forest regrowth on abandoned croplands, and tree planting for the provision of timber or fuelwood (Baumann et al., 2011; Guo et al., 2022; Townshend et al., 2012; Winkler et al., 2021). Forest losses, on the other hand, have been linked to the expansion of

agricultural and grazing lands, unsustainable wood extraction, rapid population growth, and urbanization at the expense of forestlands (FAO, 2020; Geist and Lambin, 2002; Hosonuma et al., 2012; Lambin et al., 2001; Rudel et al., 2009).

Deforestation, forest degradation, and forest fragmentation are fundamental concerns in forest conservation and management. Information on the drivers and the extent of FCC is essential for the development of appropriate forest cover restoration strategies (Agariga et al., 2021; Reddy et al., 2013). The analysis of historical trends of forest cover, structure, and temporal changes is also paramount in predicting future FCC and designing future forest management interventions for Sustainable Forest Management (SFM) (Karahalil et al., 2009). The combination of remote sensing (RS), geographical information system (GIS), and Land Use Land Cover (LULC) modelling has been recognized and used as a contemporary tool for investigating historical, present, and future changes in land and forest cover. The commonly used modelling techniques include the Cellular Automata (CA) (Kamusoko et al., 2013), Markov chain (Kumar et al., 2014), CA–Markov chain (Mengist et al., 2021; Munthali et al., 2020; Mwabumba et al., 2022; Tadese et al., 2021; Yue et al., 2024), Land Change Modeler (LCM) (Armenteras et al., 2019; Munsi et al., 2012), STCHOICE (Reddy et al., 2017), and GEOMOD (Giriraj et al., 2008; Sakieh and Salmanmahiny, 2016). These tools are vital in forest management, conservation and monitoring since they provide insights into deforestation patterns and hotspots cost-effectively and promptly (Abad-Segura et al., 2020; Alabi et al., 2021; DeFries, 2013; Dewan et al., 2012; Mishkin and Pacheco, 2022).

Land use change has increased globally over the years through the conversion of the world's forest land to other uses due to the growth of the human population and increasing demand for food and land (FAO, 2015; Lambin et al., 2001). A three-decade land cover change analysis using satellite-based observations in seven East African (EA) nations (Tanzania, Ethiopia, Kenya, Uganda, Zambia, Malawi, and Rwanda) showed a 189,400 square kilometers (km^2) decline in naturally vegetated lands comprising forests, grasslands, and wetlands (Bullock et al., 2021). A spatial analysis of Kenya's LULC changes from 1990 to 2015 revealed a 24.7% loss of forest cover between 1990 and 2000, with a subsequent 9.04% increase in forest cover between 2005 and 2015 (FAO, 2015). Results from the most recent wall-to-wall mapping of Kenya's forest resources carried out in the year 2021 showed the country's forest cover stood at 8.83% of the total land area, a rise from the previous forest cover figure of approximately 7% recorded in the year 2010 (Kenya Forest Service, 2021). This represents a significant improvement in the country's forest cover; however, existing competition from other land uses still poses a threat to Kenya's forest resources (Ministry of Environment and Natural Resources, 2016).

The Mount Kenya Ecosystem (MKE) is a designated biosphere reserve and a world heritage site in central Kenya that offers exceptional resource values of scenic, biodiversity, and cultural and social nature (Kenya Wildlife Service, 2010). It comprises forest reserves (FRs) and a national park (NP) that comprises both natural and plantation forests, providing a wide range of ecosystem services. FRs in the MKE are among the most threatened forests in Kenya due to their commercially valuable reserves of indigenous timber, and the large human population living around its land-scarce boundaries (Emerton, 1999). The MKE forests face immense pressure from human activities and natural factors, threatening its ecosystem integrity and potential to continue providing ecosystem goods and services (Kenya Forest Service, 2010; Kenya Wildlife Service, 2010; Nature Kenya, 2019).

While previous studies have documented deforestation and forest degradation in the MKE (Bussmann, 1996; Kariuki, 2006; Kinoti and Mwende, 2019), they have focused on historical periods and the isolated drivers of FCC, leaving significant gaps in understanding the implications of these changes and the interplay of natural and anthropogenic factors in forest recovery processes. Moreover, limited attention has been given to how modern technologies, community-based initiatives,

and broader policy frameworks collectively influence forest dynamics. This study addresses these gaps by providing a comprehensive analysis of historical (2000–2023) and projected FCC (2035), integrating RS and GIS methodologies with socio-environmental data. It explores the simultaneous roles of human interventions, and natural regeneration in forest recovery, offering a nuanced understanding of the drivers behind forest transitions and the socio-economic implications of the changes. Our objectives in this study are threefold. First, we detect, quantify, and map the spatio-temporal FCC trends in the MKE from 2000 to 2023 using GIS and RS. Secondly, we predict FCC for the years 2035 using the cellular automata and Markov chain analysis (CA–MCA) model, and finally, we assess the implications of these FCC on SFM in the MKE. The findings of this study will offer targeted recommendations for SFM, directly addressing the drivers of deforestation and identifying effective recovery strategies. It will further equip policymakers and conservationists with actionable insights to enhance forest resilience and carbon sequestration in similar tropical montane ecosystems.

2. Materials and methods

2.1. Study area

The MKE bestrides the equator in the central part of Kenya, spanning six administrative counties of Kirinyaga, Laikipia and Nyeri to the west and Embu, Tharaka Nithi, and Meru to the East (Fig. 1). It is geographically located within longitudes 37° 0′ and 37° 48′ E and latitudes 0° 36′ S and 0° 18′ N, covering an estimated area of about 4779.52 km^2. The MKE comprises Mt Kenya Forest Reserve (MKFR), Mt Kenya National Park (MKNP), Ngare Ndare Forest Reserve (NNFR), Lower and Upper Imenti forest reserves, Thunguru Hill Forest Reserve, Timau Forest Reserve and a 5 km buffer zone around the forested zones. The three important and closely linked forest reserves in the MKE (Mt Kenya, Ngare Ndare, and Imenti) form the core of this study (Fig. 1).

The MKE ecosystem has a bimodal rainfall pattern, with long rains occurring from March to May while short rains are experienced from October to December. Rainfall is moderate on the lower slopes and gets heavier higher up the slope. The wettest part of the mountain is to the Southeast, with up to an average of 2500 mm precipitation per year, while the Northern part of the ecosystem is the driest, with less than 1000 mm mean rainfall annually (Gichuhi et al., 2014). The altitude of the MKE ranges from 1100 m above the sea level (asl) in the Northeastern parts to 5199 m asl in the central part of the study area, which comprises the peak of Mt Kenya. The study area experiences varied temperatures ranging from about 5 °C in the upper zones, above 3000 m asl to 25 °C in the lower zones, with an average temperature reduction of about 0.6 °C for every 100 m increase in altitude. An afro-alpine climate, typical of the tropical East African high mountains, characterizes the higher ranges of the MKE (Kenya Forest Service, 2010). The dominant soils of the MKE region include Nitisols, Ferralsols, Andosols, Histosols, and Acrisols (Muchena and Gachene, 1988). The lower slopes of Mt Kenya are covered with montane forest, which includes both indigenous closed canopy and indigenous open canopy forest. The vegetation changes to bamboo, scrub, and moorland on the intermediate slopes, then to bare rock, ice, and snow on the upper slopes, with the highest point being 5199 m asl (Nature Kenya, 2019).

MKE is one of Kenya's five main water towers and is a significant water catchment for the country. Kenya's largest river, the Tana River, has its catchment area in the Northeastern to the Southwestern part of Mt Kenya, while the Ewaso Nyiro River has its catchment area in the Western and Northwestern slopes of the mountain. The Tana River provides water to several hydroelectric power plants as well as large irrigation schemes such as the Tana Delta irrigation scheme, the Mwea rice scheme, and the Bura irrigation and settlement scheme (Kenya Wildlife Service, 1999). MKE is rich in biodiversity in terms of both plant and animal species as it provides habitat to many globally threatened mammals, including the African elephant (*Loxodonta Africana*),
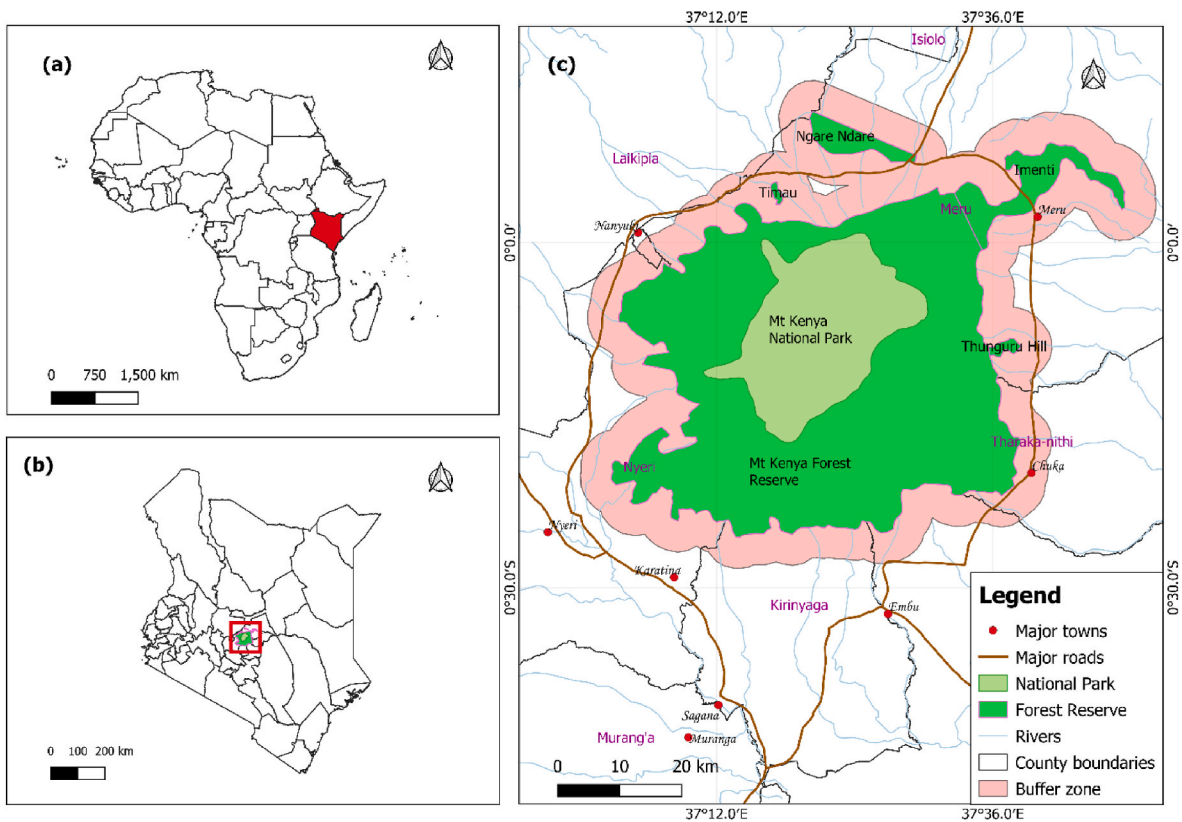
Fig. 1. Map of the study area. (a) Location of Kenya in Africa; (b) Location of MKE in Kenya; (c) Map of the MKE.

mountain bongo (*Tragelaphus eurycerus*), black-fronted duiker (*Cephalophus nigrifrons*) giant forest hog (*Hylochoerus meinertzhageni*), and the endangered king African mole rat (*Tachyoryctes rex*). An estimated 880 plant species belonging to 479 genera in 146 families have also been recorded in the ecosystem in the past (Kenya Forest Service, 2010).

Administratively, MKE is primarily managed by two government agencies, the Kenya Forest Service (KFS) and the Kenya Wildlife Service (KWS). KWS is responsible for MKNP, the innermost area (>3,200m asl), while KFS manages the MKFR and Imenti forest reserves. The NNFR is maintained by local communities, such as the Ngare Ndare Forest Trust, under the supervision of KFS (Kenya Forest Service, 2010; Kenya Wildlife Service, 2010). A predominantly agricultural production population surrounds the Mt Kenya forest reserve. The forest also provides water, wood, and non-wood forest products to the surrounding communities living within the 5 km buffer zone (Kenya Forest Service, 2015; Nature Kenya, 2019).

2.2. Data acquisition

In this study, we used two sets of data to classify the historical and predict the future LULC in the MKE. The first set was the Landsat data processed from the Google Earth Engine (GEE) platform to characterize the LULC classes within the study area. GEE delivers multi-petabyte archives of geospatial data, including satellite data, which can be used for planetary-scale analysis. Therefore, we accessed atmospherically corrected surface reflectance images for Landsat 7 Thematic Mapper, Landsat 8 OLI/TIRS, and Landsat 9 OLI-2/TIRS-2 for the years 2000, 2014, and 2023, respectively. Landsat sensors provide an extensive regular time series data for monitoring forest cover changes and other land dynamics across space and time on earth (Shravan Kumar et al., 2024). Data pre-processing involved several steps, such as filtering data by the specific season of each epoch and applying a cloud masking function to eliminate the inclusion of data with contamination effects.

Therefore, we used quality assessment bands combined with a compositing approach to only retain cloud-free pixels for further analysis. The resulting image composite was generated from the median value of the time series data analyzed in each season.

All the Landsat products used in this study were surface reflectance products which were atmospherically corrected, analysis-ready without requiring sensor-specific geometric or radiometric adjustments. Therefore, we processed spectral bands (Blue, Red, Near Infrared, Short wave infrared) and derived indices such as the Normalized Difference Vegetation Index (NDVI), Normalized Difference Bareland Index (NDBI), and Normalized Difference Moisture indices (NDMI). The formulas, references and justification for the used indices are summarized in Table 1.

The spectral bands and indices were used as input features for the subsequent supervised classification process. The bands and the indices used have shown a great potential of characterizing natural land covers and artificial environments across different environments (Allam et al., 2019; Pham-Duc et al., 2023). The bands have a spatial resolution of 30 m. The acquisition of the RS images for the different epochs was conducted within the same season of the year (Tilahun et al., 2024). This was necessary to minimize the effects of moisture and phenology

Table 1
Table showing the vegetation indices used in the study.

Vegetation Index	Formula	Justification	References
NDVI	$\dfrac{NIR - RED}{NIR + RED}$	Detects vegetation health and canopy density	(Huang et al., 2021; Rouse et al., 1974)
NDBI	$\dfrac{SWIR\,1 - NIR}{SWIR\,1 + NIR}$	Identifies bare land and impervious surfaces to assess land-use changes	(He et al., 2010; Zha et al., 2003)
NDMI	$\dfrac{NIR - SWIR}{NIR + SWIR}$	Measures vegetation moisture content and water stress in forest ecosystems	(Gao, 1996; Taloor et al., 2021)

3

differences in the utilization of images acquired in different seasons. Subsequently, we selected satellite images captured from January to March as this period coincides with the driest period in the study area, thus reducing the probability of encountering cloudy images.

The second set of data used in this article was raster maps of the spatial covariates. Spatial variables such as slope, aspect, distance to rivers, population density and proximity to roads and towns were used as factors that condition LULC changes in the region (Fig. 2). Slope and aspect variables were derived from a 30-m shuttle radar topographic mission Digital Elevation Model (DEM). The DEM was derived from the Open Topography plugin in the QGIS software by specifying the extent of the study area. Proximity to rivers, roads and towns was computed using the cost distance functions as specified by Kipkulei et al. (2022). All the conditioning surfaces were resampled to the same resolution as the RS satellite images and projected to WGS UTM Zone 37 N. The spatial covariates were used as inputs to the Modules for Land-Use Change Simulation (MOLUSCE) plugin in QGIS.

2.3. Remote sensing images processing and classification

The satellite images were processed in the GEE platform and exported as classified GeoTIFF files for final LULC change maps. The processing included classification of the raw images to obtain the dominant LULC classes of the region (Table 2). We used a supervised classification approach, where the Random Forest Classifier (RF) was adopted. The RF classifier was chosen over other classifiers for this particular study due to its effectiveness, flexibility and robustness against overfitting and outliers, its ability to handle large datasets with high dimensionality, and its capacity to provide feature importance, offering a good balance between accuracy and interpretability (Parracciani et al., 2024; Rodriguez-Galiano et al., 2012; Thonfeld et al., 2020). The algorithm is also a non-parametric machine learning language requiring no prior assumptions for the data or special considerations. The RF algorithm was parameterized by specifying a default Mtry value, which is the square root of the number of variables. We also selected 500 as the number of trees (Ntree), which has demonstrated its suitability for stabilizing the internal classification (Rotich and Ojwang, 2021). A total of 232 samples were collected for the year 2000, 230 for 2014, and 206 for 2023. Stratified random sampling was then applied within each land cover class to train and test the classifier, with 70% of the data being used for training and 30% for testing. This allocation ensured sufficient data for model training while maintaining an adequate proportion for accuracy assessment. The analysis was carried out in the GEE environment using the function *ee.Classifier.*
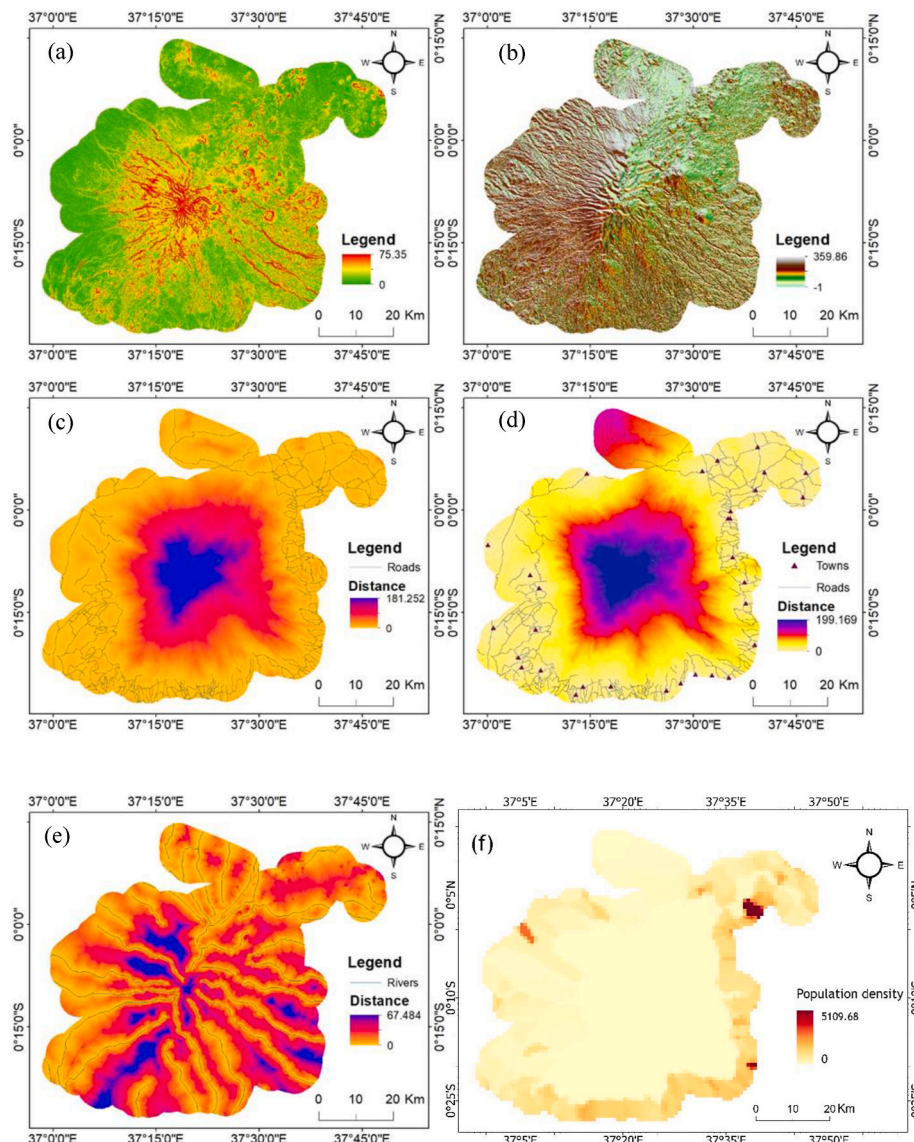

Fig. 2. LULC conditioning factors (a) Slope, (b) Aspect, (c) Proximity to roads, (d) Proximity to towns (e) Proximity to rivers and (f) Population density.

Table 2
Description of land use land cover classes in the MKE.

LULC class	Description
Cropland	Areas under annual and perennial crops.
Shrubland and grassland	Terrain adorned with miniature trees (<2m), herbaceous covers, shrubs, and bushes, occasionally intermingled with grasses, displaying a canopy cover density lower than traditional forests (<15%).
Open forest	Locations characterized by the prevalence of trees (>2m), woodlands, and bamboo with a crown cover ranging from 15 to 65%. Comprises younger regenerating forests or disturbed ecosystems, hosting a mix of pioneer and secondary species. Common species include *Croton megalocarpus*, *Dombeya torrida*, *Acacia abyssinica*, and *Arundinaria alpina*.
Closed forest	Areas characterized by the prevalence of trees (>2m), and woodlands with a crown cover above 65%. Includes old-growth or primary forests dominated by climax species. Common species include *Podocarpus latifolius*, *Prunus africana*, *Juniperus procera*, and *Ocotea usambarensis*.
Bareland	Land devoid of vegetation including rocks, snow, rough roads and temporary cultivable land which may remain uncultivated for more than one season.
Built-up area	Buildings, tarmac roads, settlements and other artificial structures that occupy the land.

smileRandomForest. GEE offers a cost-effective platform for processing voluminous satellite data therefore significantly reducing computational costs incurred in conventional download, storage and processing mechanisms (Kipkulei et al., 2022). Subsequently, the RF algorithm was trained using reference data acquired from a combination of methods such as field work, existing base maps (Topographical maps) and digitization of features from the Google Earth software using elements of interpretation such as size, texture, tone, and shapes.

2.4. Accuracy assessments

An accuracy assessment was conducted to determine the performance of the RF classifier in characterizing the LULC classes. Accuracy assessment performance is recommended in image classification to determine the robustness of the classifier in representing various earth features (Ahmed et al., 2024; Kindu et al., 2018). This study used various accuracy metrics, including the user accuracy (UA), producer accuracy (PA), F-score, kappa coefficient (K) and overall accuracy (OA).

The UA determines the proportion of corrected classified pixels in each LULC category to the total number of reference pixels in that category (row). To calculate the UA for a specific class, the number of correctly classified pixels in the corresponding column (true positives) is divided by the total number of pixels in that column from the confusion matrix, then multiplied by 100 as shown in equation (1) (Wahelo et al., 2024).

$$UA = \frac{Correctly\ classified\ pixels}{Column\ total} \times 100 \tag{1}$$

The PA determines the proportion of correctly classified pixels in each LULC category to the total number of pixels in that category (column) (Becker et al., 2021). The PA is calculated by dividing the number of correctly classified pixels by the sum of the row totals and multiplied by 100 (equation (2)).

$$PA = \frac{Correctly\ classified\ pixels}{Row\ total} \times 100 \tag{2}$$

To evaluate the accuracy of LULC classifications comprehensively, the F-score was also calculated as the harmonic mean of the PA and UA for each LULC class as depicted in equation (3) (Goutte and Gaussier, 2005; Sokolova and Lapalme, 2009). The F-score provides a balanced measure of classification performance, especially when there are imbalances between PA and UA (Powers, 2020).

$$F = 2 \times \frac{PA \times UA}{PA + UA} \tag{3}$$

Where: F = F score; PA= Producer Accuracy; UA= User Accuracy.

The K is a numerical measure of agreement between raters, factoring in the possibility of agreement occurring by chance. It contrasts the actual classification accuracy with the expected accuracy based solely on chance (Wahelo et al., 2024). The K was calculated using equation (4).

$$K = \frac{OA - EA}{1 - EA} \tag{4}$$

Where K = Kappa coefficient; OA = proportion of actual agreement between raters; EA = proportion of agreement expected by chance.

The OA is the ratio of the total number of pixels that is correctly classified to the sum of all pixels multiplied by 100 (equation (5)). It provides an overall assessment of the classification performance (Pal et al., 2013).

$$OA = \frac{Total\ number\ of\ correctly\ classified\ pixels}{Total\ number\ of\ pixels} \times 100 \tag{5}$$

2.5. Land use/landcover change analysis

The LULC change analysis was conducted to determine the proportions of changes within the LULC categories. The analysis involved determining the magnitude of change of a particular land cover in two consecutive epochs. The analysis provides a sense of growth and decline in the specific classes and allows for the interpretation of the LULC dynamics across the epochs.

The analysis was computed using Equation (6) (Blissag et al., 2024):

$$RC\ (\%) = \frac{Af - Ai}{Ai} * 100 \tag{6}$$

Where RC = % LULC rate change; Af is the area of the final year, Ai is the area of the area of the initial year.

Annual Rate of Change (ARC) analysis was also conducted using equation (7) to obtain the percentage ARC for each LULC class (Muhammad et al., 2022).

$$ARC\ (\%) = \frac{Fy - Iy}{Iy \times t} \times 100 \tag{7}$$

where *ARC* = % annual rate of change in the LULC classes; *Iy* = Initial year area; *Fy* = final year area, and *t* = time interval.

2.6. Projected LULC analysis

The LULC projection for the study region was conducted for the year 2035 under the Business as Usual (BAU) scenario. The analysis was done to inform the future LULC proportions in the study area and, hence, predict the dynamics of LULC categories in the future. The assumption in such analysis is that future LULC characterizations will be governed by transitions that have occurred in the past and interrelation between various land covers. The projected LULC for 2035 was performed using the MOLUSCE plugin in QGIS software version 2.18.24. The MOLUSCE plugin integrates some well-known algorithms for transition potential modeling, such as the artificial neural network (ANN), logistic regression, multicriteria evaluation, weights of evidence, and CA algorithm, for future simulation (Muhammad et al., 2022). The steps include adding inputs, evaluating the correlation of spatial covariates, computing area changes, transition potential modelling, CA simulation and validation. The addition of inputs requires raster files for the initial period LULC classified maps and the spatial covariates.

All the raster files should have uniform extents and the same coordinate projection and should be resampled to uniform spatial resolution.

The correlation process evaluates the relationship of geographic variables between the two raster images. In the present study, we used Pearson's correlation method. Step three on area changes computation determines the shifts of LULC between the initial and the final year specified in the inputs section. The transition potential modelling processing is the fourth step whereby the plugin uses a Multi-Layer Perception artificial neural network (MLP-ANN), Weights of Evidence (WoE), Logistic Regression (LR), and Multi-Criteria Evaluation (MCE) to calculate the potential transition maps. For the transition potential modelling, we selected a neighborhood of one pixel, a learning rate of 0.01, a momentum of 0.06, and 10 hidden layers and performed 1000 iterations. The Kappa coefficient was used to verify the accuracy of the projected LULC maps. The fifth step is CA processing, where the dynamic CA model incorporates both the spatial and temporal dimensions of the LULC classes, thereby enhancing the modelling process. The model simulates the complex interplay of time and space effects while considering the discrete nature of space, time, and state variables. The CA modelling considers the neighborhood, and thus, the proximity of the central pixel relative to the neighbors is of relative importance in assigning weights which govern the pixel changes in the future period. In this study, we evaluated Cramer's V, which is a measure of association between the LULC and the spatial drivers. The statistic varies from 0 to 1, with 1 representing a 'perfect relationship' and 0 representing 'no association'. Cramer's V is critical in choosing whether to include transition potential modelling or not, with values greater than 0.1 deemed beneficial (Muhammad et al., 2022). The final step in the LULC projection is validation, which endeavors to assess the agreement between the projected and the actual LULC. The process establishes various metrics such as the percentage of correctness, overall kappa, histogram kappa, and location kappa coefficients to assess the accuracy of the projected maps. The indices range from 0 to 1, with values close to 1 revealing a high accuracy of the prediction (Blissag et al., 2024). The methodological workflow of this study is presented in Fig. 3.

3. Results

3.1. Accuracy assessment

The accuracy metrics (producer, user, F-score, and overall accuracies) revealed a satisfactory performance of the RF classifier in characterizing LULC classes in the study region (Table 3). Producer accuracies and the F-scores were above 65%, with the built-up area depicting the lowest accuracy. Similarly, user accuracies were greater than 60% for all classes, with built-up areas revealing the same trend. Overall accuracies were 88.71% for 2000, 82.79% for 2014 and 86.62% for 2023 revealing that a high proportion of the cumulative LULC pixel classes were well characterized. The Kappa coefficient for 2000 was 0.85, 0.78 for 2014, and 0.83 for 2023 (Table 3). The performance of the RF model in depicting various classes in the study area revealed its relevance in projection analysis to explore future dynamics.

In the RF model, NDVI index, bands 2, 4, and 5 were the most important variables contributing to the characterization in variability of the LULC classes in the study area across the studied period (Fig. 4).

3.2. LULC area statistics and maps

The LULC maps (Fig. 5) and statistics (Table 4) for the MKE highlight variations in the composition and coverage of different LULC classes over the study period. In 2000, shrubland and grassland dominated the MKE landscape, covering 28.17% (1346.36 km^2), followed closely by cropland at 27.25% (1302.23 km^2). Closed forest accounted for 21.79% (1041.66 km^2), while open forest covered 19.04% (909.85 km^2). Bareland and built-up areas had the least area coverage, occupying 3.74% (179.12 km^2) and 0.01% (0.30 km^2), respectively (Table 4). By 2014, open forest emerged as the dominant LULC type, covering 30.90% (1477 km^2). Cropland followed at 28.43% (1358.68 km^2), with shrubland and grassland occupying 15.61% (746.18 km^2). The area covered by closed forest was 13.42% (641.36 km^2), while bareland comprised 11.63% (555.94 km^2) of the study area. Built-up areas remained minimal at 0.01% (0.36 km^2). In 2023, cropland became the predominant LULC class, covering 31.81% (1520.23 km^2), followed by open forest at 23.24% (1110.97 km^2) and closed forest at 18.83% (900.12 km^2). Shrubland and grassland covered 16.29% (778.43 km^2), while bareland had the second least area coverage at 9.82% (469.21 km^2). Built-up areas remained the least significant LULC category, covering 0.01% (0.57 km^2) of the MKE (Table 4).
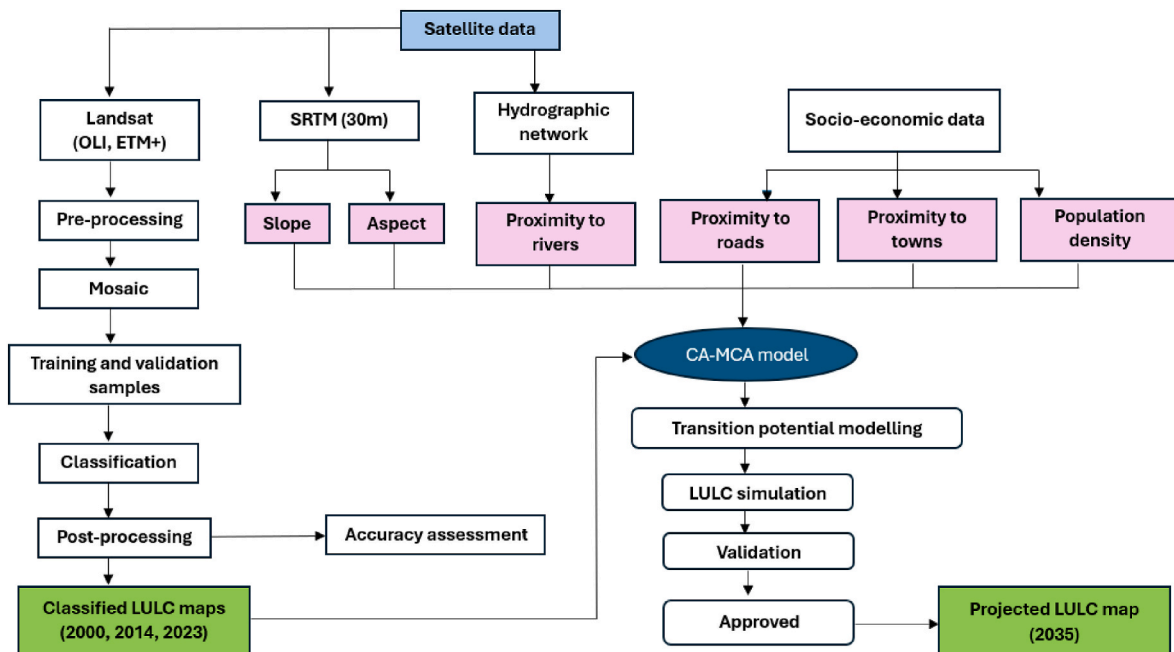

Fig. 3. Study methodology flowchart.

Table 3
Classification accuracies for the years 2000, 2014, and 2023 in the MKE.

LULC class	2000			2014			2023		
	PA	UA	F-Score	PA	UA	F-Score	PA	UA	F-Score
Open forest	93.28	92.78	93.03	88.91	91.98	90.42	87.32	97.10	91.96
Closed forest	96.68	95.69	96.18	83.44	90.30	86.74	97.35	93.49	95.38
Shrubland and Grassland	91.90	85.30	88.47	90.01	71.98	80.06	72.60	97.72	83.53
Cropland	84.57	85.19	84.88	79.98	80.66	80.32	96	73.01	83.12
Bareland	83.89	78.71	81.22	77.17	69.32	73.02	99.46	74.33	85.26
Built up area	72.86	60.00	65.54	69.98	100	82.34	65.39	100	79.06
Overall accuracy	**88.71**			**82.79**			**86.62**		
Kappa Coefficient	0.85			0.78			0.83		

Note: PA – producer accuracy, UA – user accuracy.
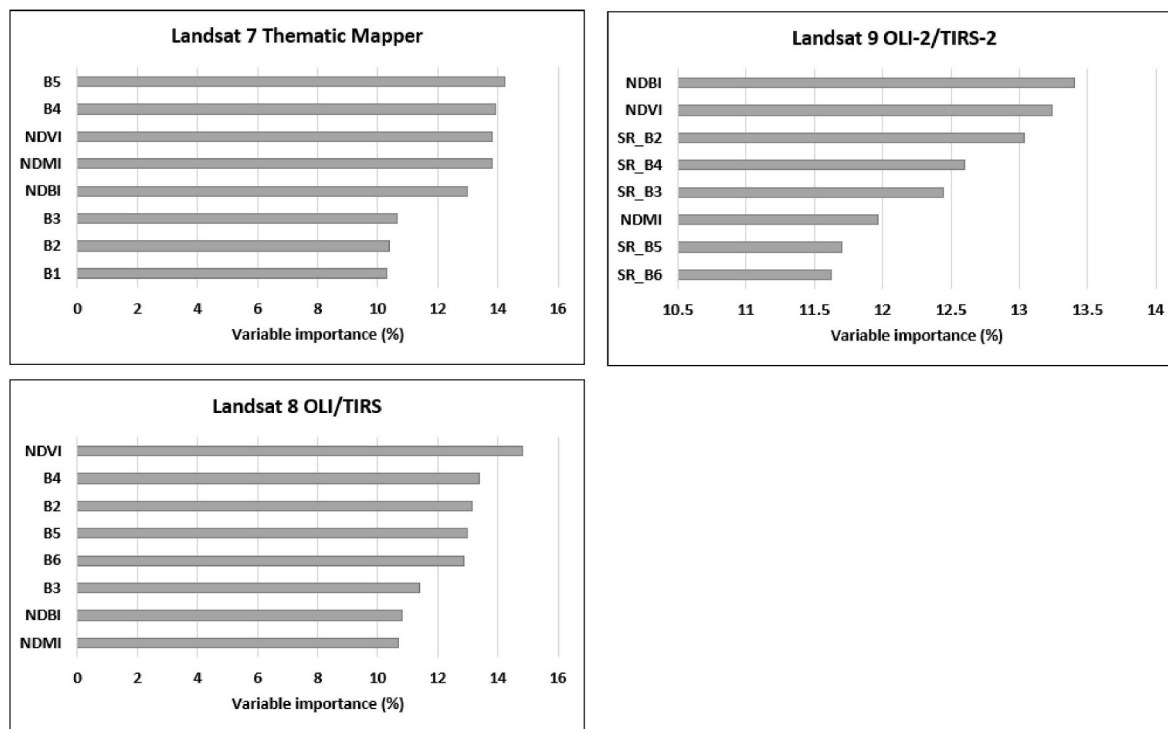
Fig. 4. Variable importance of wavelength bands for Landsat 7, Landsat 8, and Landsat 9 datasets converted into percentages.

3.3. LULC changes and annual rate of change

The analysis of LULC changes and annual rate of change (ARC) in the MKE from 2000 to 2023 revealed distinct patterns across the different LULC classes (Table 5). Open forest experienced substantial growth between 2000 and 2014, increasing by 567.15 km^2 (62.33%), followed by a decline of 366.03 km^2 (−24.78%) between 2014 and 2023, resulting in a net gain of 201.12 km^2 (22.10%) over the entire period. The ARC for open forest was 0.96% over the 23 years. Closed forest, on the other hand, saw a notable decrease of 400.31 km^2 (−38.43%) from 2000 to 2014, followed by a recovery of 258.76 km^2 (40.35%) from 2014 to 2023, leading to an overall loss of 141.55 km^2 (−13.59%). Closed forest had an annual decline rate of −0.59%.

Shrubland and grassland exhibited a decline from 2000 to 2014, losing 600.17 km^2 (−44.58%), followed by a minor increase of 32.25 km^2 (4.32%) from 2014 to 2023. This culminated in a net reduction of 567.93 km^2 (−42.18%) over the study period. Shrubland and grassland had the highest annual decline rate with the ARC averaging −1.83%. Cropland expanded steadily, gaining 56.45 km^2 (4.33%) between 2000 and 2014 and 161.55 km^2 (11.89%) between 2014 and 2023, amounting to a total increase of 218.00 km^2 (16.74%). The cropland annual growth rates were modest, at 0.73%. Bareland exhibited dramatic changes,

expanding by 376.82 km^2 (210.36%) from 2000 to 2014 before shrinking by 86.73 km^2 (−15.60%) from 2014 to 2023, resulting in a net gain of 290.09 km^2 (161.94%). Bareland had the highest annual growth rate with an average ARC of 7.04% over the 23 years. Built-up areas, while occupying the smallest area, displayed consistent growth, with an increase of 0.07 km^2 (23.39%) between 2000 and 2014 and 0.20 km^2 (55.77%) between 2014 and 2023. This resulted in an overall increase of 0.27 km^2 (92.20%) over the study period, with an ARC of 4.01% (Table 5). The LULC gains and losses in the MKE are presented in Fig. 6.

We used a Sankey plot (Fig. 7) to depict the dynamics of LULC changes in the two epochs. A Sankey plot provides an intuitive visualization of the LULC transformations. The LULC coverage for specific years is represented by nodes, with the heights showing the relative size of the LULC class within the whole graph. The nodes are interconnected with links that depict a flow from one set of values to another. Notable transformations in the MKE include changes from bareland to cropland, shrubland and grassland to cropland, shrubland and grassland to open forest, closed forest to open forest and vice versa, and cropland to open forest and vice versa. In the first epoch, the closed forests were largely converted to open forests, while shrubland and grasslands were majorly converted to croplands (Fig. 7). Croplands were transformed into bareland, shrubland and grassland, and open forest in different
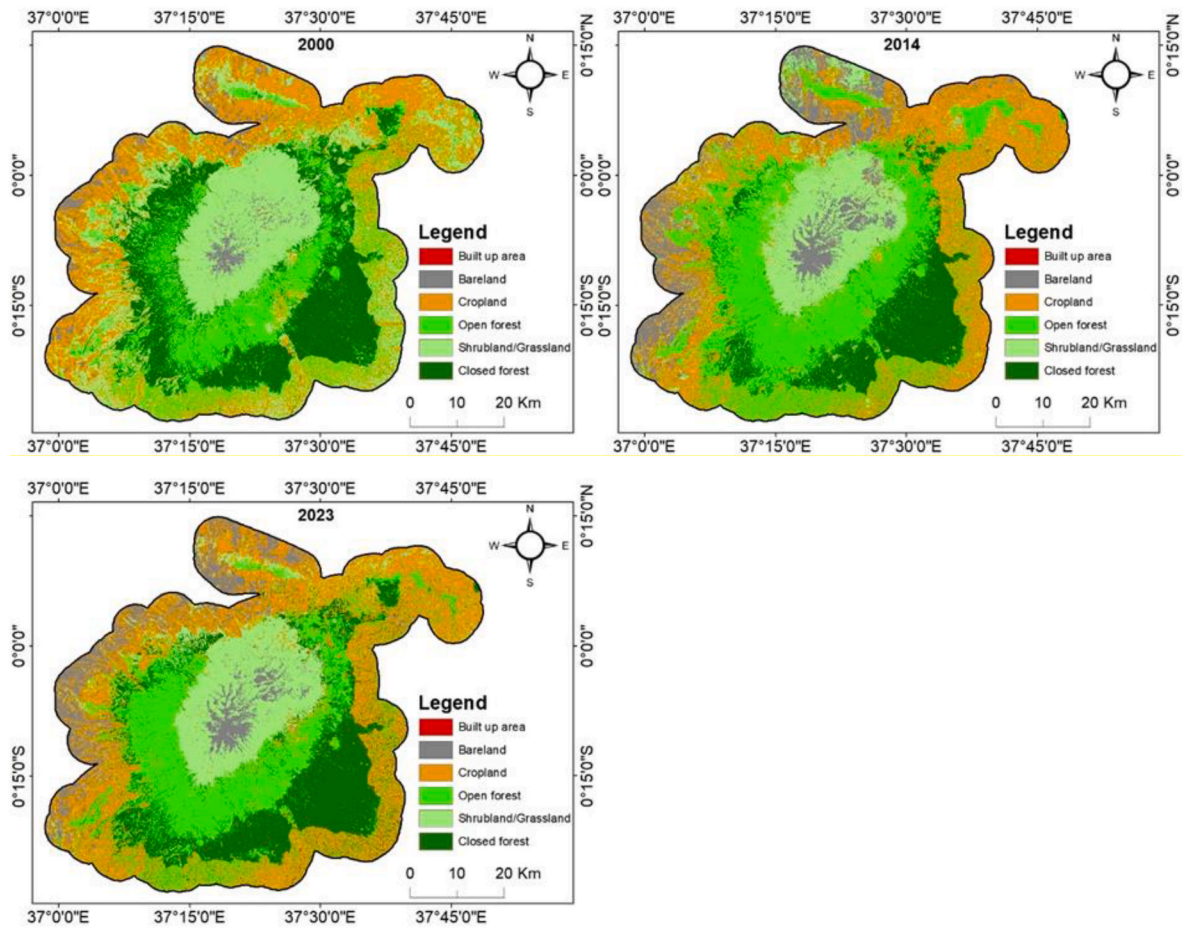
Fig. 5. LULC maps of the MKE for the years 2000, 2014, and 2023.

Table 4
LULC statistics for the years 2000, 2014 and 2023 in the MKE.

LULC classes	2000		2014		2023	
	km^2	%	km^2	%	km^2	%
Open forest	909.85	19.04	1477.00	30.90	1110.97	23.24
Closed forest	1041.66	21.79	641.36	13.42	900.12	18.83
Shrubland and Grassland	1346.36	28.17	746.18	15.61	778.43	16.29
Cropland	1302.23	27.25	1358.68	28.43	1520.23	31.81
Bareland	179.12	3.74	555.94	11.63	469.21	9.82
Built-up area	0.30	0.01	0.36	0.01	0.57	0.01
Total	**4779.52**	**100**	**4779.52**	**100**	**4779.52**	**100**

magnitudes. In the second epoch, open forest was converted to closed forests and cropland while bareland were transformed into cropland. Cropland changes were not dominant, except for some areas converted to open forests and bareland (Fig. 7).

3.4. Selection of spatial variables, projected LULC simulation and map

The LULC dynamics investigation was based on physical and socio-economic drivers. Slope, aspect, proximity to roads, proximity to rivers, population density, and proximity to market centers/towns were used as spatial covariates to simulate the future LULC changes in the study area. Table 6 shows the prospective Cramer's V value of each spatial variable. Cramer's V value suggests that the variables were ideal for transition potential modeling, as all their values were significant (>0.1). Human-related factors including proximity to towns (0.62) and population density (0.57) were the most significant drivers of LULC changes in the

Table 5
LULC changes and annual rate of change in the MKE.

LULC classes	LULC changes						ARC
	2000–2014		2014–2023		2000–2023		2000–2023
	km^2	%	km^2	%	km^2	%	%
Open forest	567.15	62.33	−366.03	−24.78	201.12	22.10	0.96
Closed forest	−400.31	−38.43	258.76	40.35	−141.55	−13.59	−0.59
Shrubland and Grassland	−600.17	−44.58	32.25	4.32	−567.93	−42.18	−1.83
Cropland	56.45	4.33	161.55	11.89	218.00	16.74	0.73
Bareland	376.82	210.36	−86.73	−15.60	290.09	161.94	7.04
Built-up area	0.07	23.39	0.20	55.77	0.27	92.20	4.01

Note: ARC– Annual rate of change (%).

Fig. 6. LULC gains and losses in the MKE.

MKE, with proximity to roads (0.49) also playing a significant role. Slope, rivers and aspect were also significant but had a relatively lesser influence on LULC changes in this study (Table 6). These simulations were conducted over a decade to obtain likely LULC characterizations in 2035. Before the projection, the capability of the CA-Markov projection model was assessed by comparing the observed and the predicted LULC map for the year 2023. The observed and simulated LULC were validated and visualized using the multiple-resolution budget displayed in Fig. 8. The validation statistics revealed good agreement between the observed and the predicted map of the MKE. The kappa (histogram) of 0.84, the kappa (overall) of 0.78, the kappa (location) of 0.84, and the % of correctness of 81.87% all point to a promising agreement between forecasted and observed 2023 LULC conditions. This indicates that the model is performing well for the MKE ecosystem watershed.

The overall Kappa coefficient value of 0.78 and an accuracy of 82% indicated good results for LULC changes and projected maps for 2035.

Based on the change percentage of area in the studied epochs, the transition potential modeling was conducted using a Multi-layer perceptron Artificial Neural Network (MLP-ANN) to forecast the LULC classes in the MKE. The ANN learning curve is indicated in Fig. 9a and the projected LULC map is in Fig. 9b. Upon validation of the model, prediction of future LULC for the MKE was conducted.

3.5. LULC statistics, changes and annual rate of change for 2035

The projection statistics for the year 2035 revealed varied trends in the various LULC classes under the BAU scenario. Open forest is expected to increase substantially by 471.72 km^2 (42.46%), with an ARC of 3.54%. Conversely, closed forest is projected to decline sharply by -423.53 km^2 (-47.05%), at an ARC of -3.92%, highlighting ongoing pressures on dense forest cover. Similarly, shrubland and grassland are anticipated to decrease significantly by -357.79 km^2 (-45.96%), with an ARC of -3.83% (Table 7).

Cropland, a dominant LULC class, is projected to expand moderately by 174.70 km^2 (11.49%), with an ARC of 0.96%, reflecting continued agricultural intensification. Bareland is also expected to increase by 134.40 km^2 (28.64%), with an ARC of 2.39%, indicating potential land degradation or exposure. While the built-up area will remain a minor category in overall coverage, it is predicted to grow rapidly by 0.49 km^2

Table 6
Cramer's V values of spatial variables.

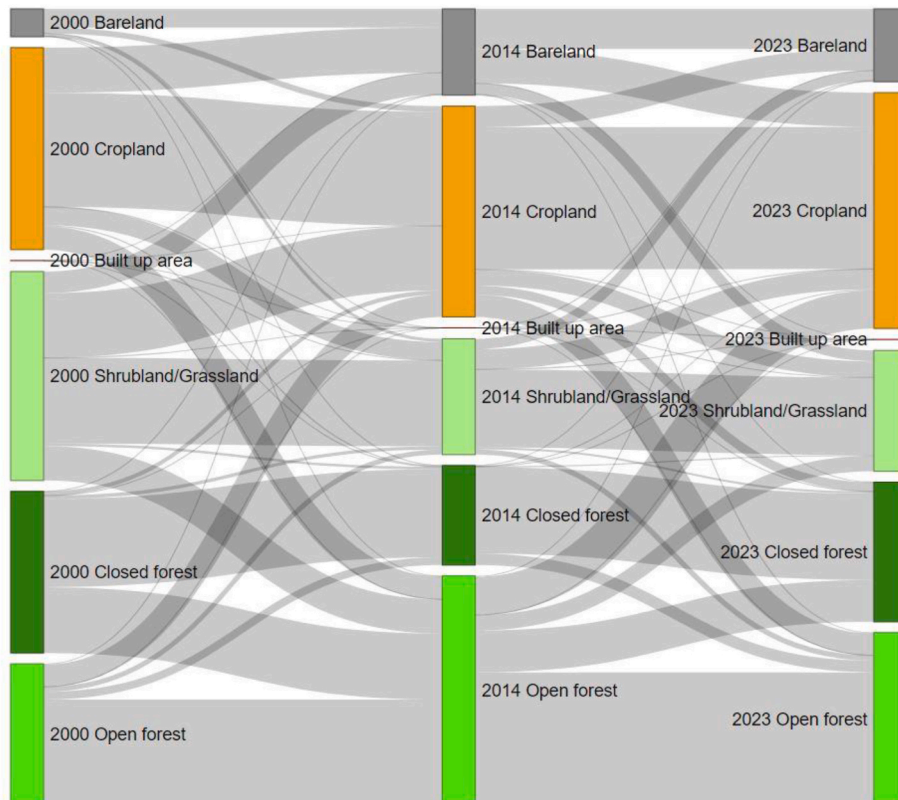| Spatial Variables	Cramer's V
Slope	0.19
Aspect	0.16
Population density	0.57
Proximity to roads	0.49
Proximity to rivers	0.32
Proximity to towns	0.62

Fig. 7. Sankey plot showing LULC transformations in the MKE.
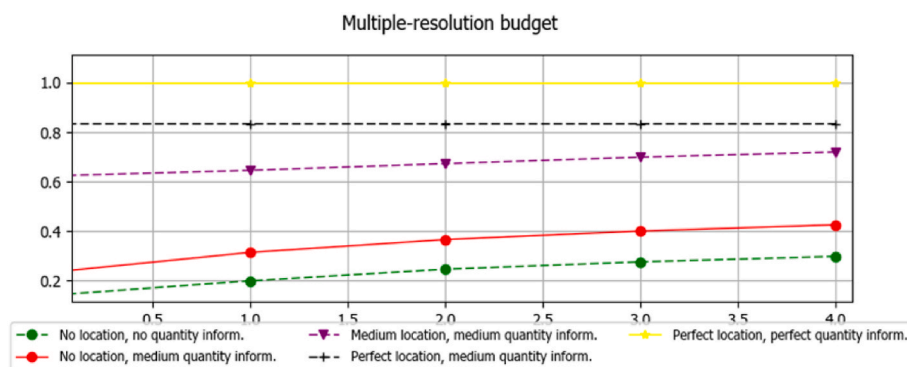
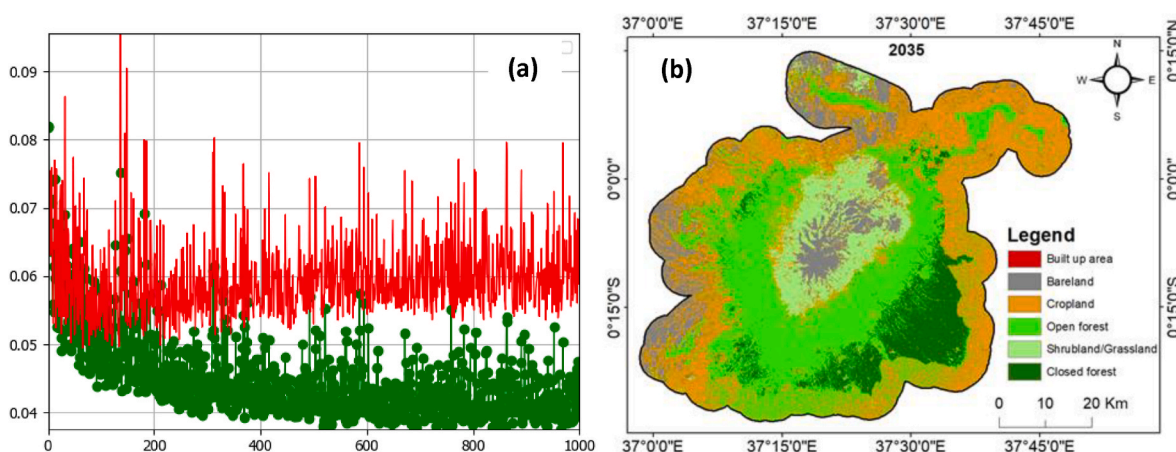Fig. 8. Validation graph between observed 2023 and predicted 2023 LULC map.

Fig. 9. (a) ANN learning curve and (b) projected LULC map for 2035.

Table 7
Predicted LULC statistics for 2035 and LULC changes (2023–2035) in the MKE.

LULC classes	LULC 2035		LULC changes 2023–2035		ARC 2023–2035
	km²	%	km²	%	%
Open forest	1582.69	33.12	471.72	42.46	3.54
Closed forest	476.59	9.97	−423.53	−47.05	−3.92
Shrubland and Grassland	420.65	8.80	−357.79	−45.96	−3.83
Cropland	1694.94	35.46	174.70	11.49	0.96
Bareland	603.61	12.63	134.40	28.64	2.39
Built-up area	1.06	0.02	0.49	86.07	7.25
Total	**4779.52**	**100**			

(86.07%), with an ARC of 7.25%, signaling accelerated urbanization trends (Table 7).

4. Discussion

4.1. Historical LULC change patterns

Based on the study findings, it is apparent that the MKE has undergone various changes in recent years, which are driven by both human and natural influences. The analysis shows that agricultural land appeared to have increased coverage in the two studied epochs. This finding is in line with past studies in the Mt. Kenya region, which have documented agricultural encroachment and intensification caused by changing demographics and agricultural ventures in the region (Eckert et al., 2017; Notter et al., 2007). The earlier studies confirmed increased agricultural intensification at the beginning of the century in the

foothills of Mt. Kenya, which lies squarely within the ecosystem. Similarly, other studies have found intensified commercial horticulture in regions surrounding Mt. Kenya in recent decades (Muriithi, 2016). Likewise, studies in Kenya focusing on land use dynamics in sensitive environments, especially water towers, have shown rapid expansion of croplands at the expense of other LULC types (Jebiwott et al., 2021; Kipkulei et al., 2022; Rotich et al., 2022; Sitati et al., 2024). These areas have been put under the production of various horticultural produce by national and multi-national companies, with both rainfed and irrigated farming intensively practiced (Ministry of Agriculture Livestock and Fisheries, 2017; The county government of Meru, 2018).

Various factors have also contributed to forest cover dynamics. The decline in closed forest cover in the first epoch (2000–2014) can be attributed to deforestation and forest degradation mainly driven by human activities in the form of encroachment for agricultural activities, illegal timber logging, firewood collection, forest fires, marijuana (*Cannabis sativa*) cultivation and charcoal production (Bussmann, 1996; Kariuki, 2006; Kenya Forest Service, 2010; Nature Kenya, 2019; Nyongesa and Vacik, 2018). A surveillance conducted by the KWS revealed encroachment by smallholder agriculture in the lower fringes of MKFR, while cultivation of *Cannabis sativa* was evident deep inside the forest (Kenya Wildlife Service, 1999). The MKE experiences frequent forest fires dating back to at least 26,000 years which in most cases, are set by humans accidently or intentionally (Henry et al., 2019). The Major causes of forest fires in the MKE include charcoal burners, honey collectors, arsonists, cigarette smokers, cattle grazers and hunters (Nyongesa and Vacik, 2018). The dense population around the MKFR often encroach into the forest for timber logging, firewood collection and charcoal production as the latter two are the major energy sources for most households in the region (Kenya Forest Service, 2010, 2015).

In the later epoch (2014–2023), closed forest coverage increased due to various reasons including natural forest regeneration, broader policy initiatives, fencing the ecosystem, intensified surveillance, community involvement, monitoring and enforcement, and the use of modern technologies in forest alerts (Kenya Forest Service, 2015; Kinyili, 2023a). First, the responsible agencies managing the MKE ecosystem (KFS, KWS) improved the enforcement of the ban on illegal activities in the forest, reducing the rate of deforestation (Kinoti and Mwende, 2019). Secondly, community involvement in conservation activities through the Community Forest Associations (CFAs) largely contributed to the improved state of the natural forest in the ecosystem (Downing et al., 2023). Other studies show that the communities surrounding the MKE had positive perceptions of forest conservation and are slowly developing a positive attitude towards protecting the forests through fencing (David Mbuba, 2019; Kinyili, 2023b). Although it is difficult to quantify the influence of these community initiatives, studies show that locally adapted strategies and conservation efforts of communities exert a lot of influence on the trajectory efforts and course of natural environments in other regions (Reed et al., 2019; Surya et al., 2020). Furthermore, other initiatives, including the International Small Group and Tree Planting Program (TIST), have realized positive greening trends in the MKE through their financial incentives to farmers integrating trees into their farms. The increased closed forest area can also be partly credited to the ongoing fencing of Mt Kenya forest which was launched in 2012 and spearheaded by the Rhino Ark Trust, a charitable conservation organization, in partnership with the Kenya Forest Service, Kenya Wildlife Service, Space for Giants, Mount Kenya Trust, and the British Army Training Unit Kenya (Kenya Forest Service, 2021). Phase one of the fencing comprising a 50 km stretch of electric fence covering sections of the MKE in Kirinyaga and Embu counties has already been completed with phase two covering Tharaka Nithi and Meru counties set to commence soon. In total, the 450 km long perimeter fence aims to border off 2700 km^2 of the MKE upon completion which will further reduce encroachment into the forest and incidences of human-wildlife conflicts in the study area (Kenya Forest Service, 2021).

The increase in closed forest area in the second epoch can also be attributed to natural forest regeneration in previously degraded forest areas as a result of reduction in disturbances from illegal logging and encroachment for agriculture following improved monitoring, enforcement, and the use of modern technologies in forest alerts (Kinyili, 2023a). The region's favorable climatic conditions in the form of increased precipitation in the second study period also played a significant role in forest recovery (Jia et al., 2024; Schmocker et al., 2016). Broader policy initiatives at the national and regional levels, such as Kenya's commitment under the African Forest Landscape Restoration Initiative (AFR100) and projects like the Mount Kenya Forest Restoration Program, have been pivotal in increasing tree cover between 2014 and 2023. These programs focus on replanting indigenous tree species to promote MKE recovery, and enhance biodiversity (Kenya Forest Service, 2021).

Changes in other land cover over the epochs are also attributed to human influences. For instance, the surge in bareland areas in the first epoch might be due to deforestation, overgrazing, and agricultural land degradation resulting from unsustainable land use practices (Maina and Nzengya, 2021; Nature Kenya, 2019). Encroachment into forested and vegetated areas for charcoal production, subsistence farming, and construction likely exacerbated land cover changes, leaving vast areas bare. In addition, localized natural events such as droughts which occurred between 2008 and early 2010 and high intensity of fires during the period notably in the year 2012 could have intensified land degradation, hence increased bareland areas (County Government of Tharaka Nithi, 2023). Wildfires are common in mountainous regions and their surroundings especially during the dry season due to their rich biomass (Poletti et al., 2019; Rotich et al., 2020). The decline in the shrubland areas is a result of an increase in bareland, open forests, and cropland areas. These changes appear to be the key transformations occurring in

the class. The finding is in line with other studies covering part of the ecosystem, which revealed a decline in shrubland areas during the study period (Gichuhi et al., 2014; Sang et al., 2023).

The rapid increase in the built-up areas throughout the study period and specifically in the first study period (2000–2014) aligns with broader regional trends and socio-economic factors. Built-up areas expanded due to steady population growth in all the six study counties (Fig. 10) and urban sprawl, driven by rural-to-urban migration and infrastructure development in regions bordering the MKE. Increased population leads to increased settlements and growth of trading and urban centers. This finding aligns with that by Shukla et al. (2018), who identify population growth as the primary driver behind industrialization, gradual urbanization, infrastructural development and agricultural intensification in the Upper Ganga River basin of India. The devolution of most national government functions to the County level after the promulgation of the new constitution in the year 2010 has also triggered industrial and infrastructural development in the relevant counties hence the observed increase in built-up areas (Embu County Government, 2019).

4.2. Projected LULC change patterns

Based on the historical LULC dynamics, projections for the MKE ecosystem reveal varied trajectories for different LULC classes. The findings indicate that built-up areas, bareland, grasslands, and open forests are expected to expand. These projected trends align with ongoing processes of agricultural intensification, urbanization, and deforestation, which have historically driven LULC changes globally (Hou et al., 2022). The anticipated growth of built-up areas mirrors global trends, where urbanization increasingly encroaches on croplands and natural ecosystems such as forests and pastures (Muhammad et al., 2022; Nayak et al., 2024). Urban sprawl, driven by population growth and socio-economic development, leads to the conversion of rural and peri-urban landscapes into urban footprints (Biney and Boakye, 2021; Biswas et al., 2020; Munthali et al., 2020). This trend is also visible in Kenya, where expanding urban centers and infrastructure projects compete with other land uses (Kipkulei et al., 2022; Kogo et al., 2021; Rotich et al., 2022). Similarly, the projected expansion of bareland reflects land degradation processes exacerbated by deforestation, overgrazing, and changing climatic conditions. Comparable multi-decadal studies in Zambia and Ethiopia have similarly documented bareland increases at the expense of grasslands and forests (Chisanga et al., 2023; Kindu et al., 2018).

Closed forest cover is expected to decline further, likely transitioning into open forest due to ongoing deforestation and forest degradation. The reduction of closed forests underscores the need for urgent conservation efforts. Current initiatives, such as Kenya's ambitious plan to
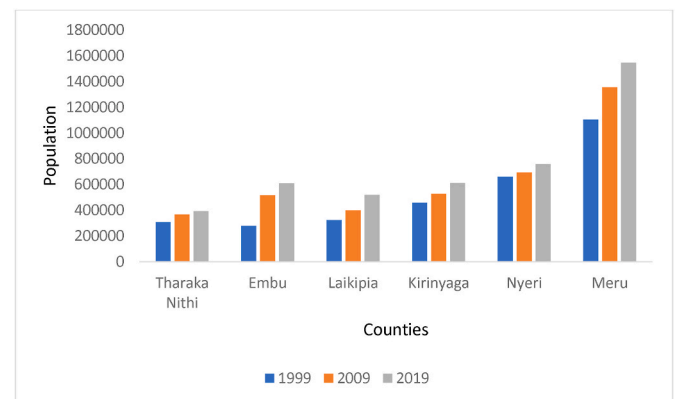
Fig. 10. Human population trends in the six MKE counties (Kenya National Bureau of Statistics, 2019).

plant 15 billion trees by 2032 under the African Landscape Restoration Initiative, represent critical steps toward reversing forest loss (Kenya Forest Service, 2021). However, without robust enforcement and community engagement, these efforts may struggle to offset deforestation drivers such as illegal logging and land conversion for agriculture.

Shrubland and grassland areas are projected to decrease, driven by increasing demand for arable land to support the ever-growing population (County Government of Tharaka Nithi, 2023). The competition between food security and ecosystem conservation remains a pressing challenge globally and in the MKE region (Jouzi et al., 2022; Kenya Forest Service, 2010). To make these projections actionable for policymakers, it is essential to integrate considerations of ongoing conservation programs, climate adaptation strategies, and socio-economic plans specific to the MKE region. Enhancing the capacity of community-based forest management programs, promoting sustainable agriculture, and investing in climate-resilient land-use planning could help mitigate the adverse impacts of the LULC changes. By aligning these projections with regional development goals, this study can provide a framework for balancing economic growth with ecological sustainability in the MKE.

4.3. Implications for sustainable forest management and conservation

The MKE exemplifies one of the crucial natural resources in Kenya, with huge significance to important sectors such as forestry, water, and tourism. The dynamics of LULC and the projected LULC changes are likely to induce landscape alterations at various magnitudes. The changes will have profound impacts on terrestrial gross productivity, provision of ecosystem services, biodiversity and the exchange of water, energy, and carbon fluxes if the trend continues unchecked.

The MKFR is crucial for carbon sequestration, water balance, and biodiversity conservation. Deforestation and forest degradation translate to loss of the carbon sequestration value of land and contribute to global emissions hence climate change (Reay et al., 2007). The MKE appears in the United Nations Educational, Scientific and Cultural Organization (UNESCO) World Heritage list. It is also a vital biosphere reserve (Kenya Forest Service, 2010). If the decline in the forest area is not checked, there is a likelihood of future collapse of the whole ecosystem and its capacity to generate goods and services such as food, water, medicinal herbs, and timber.

Encroachment and destruction of the forest is a threat to wildlife habitat and biodiversity. A study by Fundi (2020) notes that farming, timber extraction, grazing and access to firewood are detrimental to wildlife habitat and are bound to affect the reintroduced endangered endemic mountain bongo (*Tragelaphus eurycerus isaaci*) population. A comparative study in the MKE also established that natural forests had the highest overall avian species richness and relative species richness compared to plantation forests and farmlands (Mahiga et al., 2019). The feedback loop related to declining wildlife habitat might cause extirpation of certain key organisms like honeybees, butterflies and other insects that play the critical role of pollination due to the conversion of grasslands and shrublands and forestland into cropland and settlements thereby promoting treeless landscapes as it is in the current situation. This might further lead to loss of livelihoods for residents by degradation of scenery characteristics of the region and its potential to attract tourists. The loss of grassland may lead community members to put more pressure on the remaining forest land for grazing, resulting in a further loss of forestland.

Agricultural expansion in the highland zones of the MKE results in the over-abstraction of water from rivers and streams for irrigation purposes (Wiesmann et al., 2000; Zaehringer et al., 2018). This results in water scarcity in the lower dry areas like the Laikipia plateau setting the stage for increased conflicts over water resources (Wiesmann et al., 2000). Water quality is likely to be negatively impacted by discharges from the agricultural fields emanating from the use of inorganic fertilizers, pesticides and herbicides. A study in the upper Ganga basin of India similarly reported water pollution due to agricultural practices,

mainly fertilizers (Shukla et al., 2018). Destruction of forests which is a key water catchment also reduces the water flow downstream and results in increased soil erosion and land degradation (Zaehringer et al., 2018). Basha et al. (2024) assert that clearing of forests for farming activities may result in negative effects, such as low infiltration rates, increased water yield and surface runoff, and a reduction in accessible groundwater from wells and reservoirs.

Encroachment into the forest also threatens the co-existence of human and wildlife populations in the region. This is evident through frequent incidences of human-wildlife conflict reported in the area due to settlement in the wildlife movement corridors and utilization of the buffer areas adjacent to the protected areas in the region (Kiria et al., 2019). Animal incursions on nearby farmlands are identically common due to the proximity of human settlements to the MKE (Kenya Wildlife Service, 2010).

4.4. Recommendations for resource managers and policymakers

From this research, it is evident that the sustainable management of MKE forests is not only vital for biodiversity conservation and ecosystem services but also for the livelihoods and well-being of local communities. The following measures therefore ought to be taken to achieve SFM.

- Increase community-based surveillance and stricter implementation and enforcement of forest laws and penalties to curb illegal logging, marijuana (*Cannabis sativa*) cultivation and charcoal production in the Mount Kenya forest.
- Subsidize and distribute alternative energy sources, such as solar cookers and biogas, to reduce overdependence on firewood and charcoal. Encourage residents in the MKE to adopt energy-efficient cooking stoves to reduce firewood and charcoal consumption.
- Adequate allocation of financial, human, and technological resources to support forest monitoring, data collection, and management activities is imperative. Adequate resources are fundamental for the completion of the remaining 400 km perimeter fence around the MKFR to help maintain the integrity of the ecosystem.
- Initiate large-scale reforestation and afforestation programs in the MKE to restore degraded forest areas and expand forest cover. Planting of native tree species like *Podocarpus latifolius* and *Juniperus procera* that are well-suited to the local ecological conditions and contribute to biodiversity conservation should be prioritized.
- Enhancing collaboration and partnerships among government agencies, research institutions, civil society organizations, and local communities in the MKE region is vital for a comprehensive approach to forest management. Joint initiatives will facilitate data sharing, joint monitoring efforts, and collaborative research, ultimately enhancing collective understanding of forest dynamics.
- Encourage the adoption of agroforestry practices among the local farmers to promote sustainable land use while maintaining forest cover. Provide training, technical support, and incentives to farmers for implementing agroforestry systems that integrate trees with crop and livestock production to reduce their overdependence on the forest for timber, building poles, charcoal and firewood.
- Deploy remote sensing and GIS technologies for real-time fire monitoring and early warning, establish and maintain firebreaks in fire hotspot areas, and provide adequate equipment and training for forest rangers and community members in the MKE to ensure swift and efficient responses to forest fires.
- Encourage sustainable tourism practices that support local livelihoods while minimizing negative impacts on the environment in the MKE. Develop ecotourism initiatives that raise awareness about the importance of forest conservation and generate revenue for conservation efforts.

5. Conclusions

The current study is the first attempt to quantify and map historical and projected FCC in the MKE, central Kenya using RS, GIS, and the CA-MCA modeling techniques. Results revealed significant LULC changes over the past two decades, including expansion of cropland, built-up areas, and open forest, alongside declines in closed forest coverage. Projected analysis suggests that under the BAU, these trends are likely to persist.

These trends highlight the urgent need for proactive management measures to mitigate further degradation and deforestation and enhance forest recovery in the MKE, given its ecological significance. This study outlines the interplay of natural and anthropogenic factors in forest cover dynamics, and serves as a call to action, urging policymakers, practitioners, and citizens to prioritize the protection and sustainable management of MKE. By delivering actionable insights for sustainable forest management and linking findings to global conservation priorities, this study advances the current knowledge on tropical montane ecosystems and their role in mitigating climate change.

Recommendations outlined in the study emphasize the need for improved resources allocation, enhanced collaboration, capacity building, and technological innovation to strengthen forest monitoring, management, and conservation efforts. By implementing the recommendations outlined in this study, Kenya can forge a path towards a more resilient, equitable, and environmentally sustainable future. We further recommend future studies in the MKE on how these LULC changes affect carbon stock dynamics.

CRediT authorship contribution statement

Brian Rotich: Writing – review & editing, Writing – original draft, Investigation, Conceptualization. **Abdalrahman Ahmed:** Writing – original draft, Methodology, Formal analysis. **Benjamin Kinyili:** Writing – review & editing, Writing – original draft. **Harison Kipkulei:** Writing – review & editing, Writing – original draft, Visualization, Validation, Software, Methodology.

Funding

Declaration of competing interest

The authors declare that they have no known competing financial interests or personal relationships that could have appeared to influence the work reported in this paper.

Acknowledgements

Data availability

Data will be made available on request.

References

Abad-Segura, E., González-Zamar, M.D., Vázquez-Cano, E., López-Meneses, E., 2020. Remote sensing applied in forest management to optimize ecosystem services: advances in research. Forests 11. https://doi.org/10.3390/f11090969.

Agariga, F., Abugre, S., Appiah, M., 2021. Spatio-temporal changes in land use and forest cover in the asutifi north district of ahafo region of Ghana , (1986 – 2020). Environ. Challenges 5, 100209. https://doi.org/10.1016/j.envc.2021.100209.

Ahmed, A., Rotich, B., Czimber, K., 2024. Assessment of the environmental impacts of conflict-driven Internally Displaced Persons: a sentinel-2 satellite based analysis of land use/cover changes in the Kas locality, Darfur, Sudan. PLoS One 19, 1–19. https://doi.org/10.1371/journal.pone.0304034.

Alabi, K., Tobore, A., Oyerinde, G., Senjobi, B., 2021. Forest cover change in Onigambari reserve , Ibadan , Nigeria : application of vegetation index and Markov chain techniques. Egypt. J. Remote Sens. Sp. Sci. 24, 983–990. https://doi.org/10.1016/j.ejrs.2021.08.004.

Allam, M., Bakr, N., Elbably, W., 2019. Multi-temporal assessment of land use/land cover change in arid region based on landsat satellite imagery: case study in Fayoum Region, Egypt. Remote Sens. Appl. Soc. Environ. 14, 8–19. https://doi.org/10.1016/j.rsase.2019.02.002.

Armenteras, D., Murcia, U., González, T.M., Barón, O.J., Arias, J.E., 2019. Scenarios of land use and land cover change for NW Amazonia: impact on forest intactness. Glob. Ecol. Conserv. 17. https://doi.org/10.1016/j.gecco.2019.e00567.

Balthazar, V., Vanacker, V., Molina, A., Lambin, E.F., 2015. Impacts of forest cover change on ecosystem services in high Andean mountains. Ecol. Indic. 48, 63–75. https://doi.org/10.1016/j.ecolind.2014.07.043.

Basha, U., Pandey, M., Nayak, D., Shukla, S., Shukla, A.K., 2024. Spatial–temporal assessment of annual water yield and impact of land use changes on upper Ganga basin, India, using InVEST model. J. Hazardous, Toxic, Radioact. Waste 28. https://doi.org/10.1061/jhtrbp.hzeng-1245.

Baumann, M., Kuemmerle, T., Elbakidze, M., Ozdogan, M., Radeloff, V.C., Keuler, N.S., Prishchepov, A.V., Kruhlov, I., Hostert, P., 2011. Land use policy patterns and drivers of post-socialist farmland abandonment in western Ukraine. Land Use Policy 28, 552–562. https://doi.org/10.1016/j.landusepol.2010.11.003.

Becker, W.R., Ló, T.B., Johann, J.A., Mercante, E., 2021. Statistical features for land use and land cover classification in Google Earth Engine. Remote Sens. Appl. Soc. Environ. 21, 100459. https://doi.org/10.1016/j.rsase.2020.100459.

Biney, E., Boakye, E., 2021. Urban sprawl and its impact on land use land cover dynamics of Sekondi-Takoradi metropolitan assembly, Ghana. Environ. Challenges 4, 100168. https://doi.org/10.1016/j.envc.2021.100168.

Biswas, M., Banerji, S., Mitra, D., 2020. Land-use–land-cover change detection and application of Markov model: a case study of Eastern part of Kolkata. Environ. Dev. Sustain. 22, 4341–4360. https://doi.org/10.1007/s10668-019-00387-4.

Blissag, B., Yebdri, D., Kessar, C., 2024. Spatiotemporal change analysis of LULC using remote sensing and CA-ANN approach in the Hodna basin, NE of Algeria. Phys. Chem. Earth 133, 103535. https://doi.org/10.1016/j.pce.2023.103535.

Bullock, E.L., Healey, S.P., Yang, Z., Oduor, P., Gorelick, N., Omondi, S., Ouko, E., Cohen, W.B., 2021. Three decades of land cover change in East Africa. Land 10, 1–15. https://doi.org/10.3390/land10020150.

Bussmann, R.W., 1996. Destruction and management of mount Kenya's forests. Ambio 25, 314–317.

Chisanga, C., Phiri, D., Harnadih Mubanga, K., 2023. Multi-decade land cover/land use dynamics and future predictions for Zambia: 2000 - 2030. Discov. Environ. https://doi.org/10.1007/s44274-024-00066-w.

County Government of Tharaka Nithi, 2023. THIRD COUNTY INTERGRATED DEVELOPMENT PLAN, 2023-2027).

David Mbuba, M., 2019. Fencing and forest conservation: attitudes of local people living adjacent to eastern slopes of mount Kenya. Int. J. Nat. Resour. Ecol. Manag. 4, 1. https://doi.org/10.11648/j.ijnrem.20190401.11.

DeFries, R., 2013. Why forest monitoring matters for people and the planet. Global Forest Monitoring from Earth Observation.

Dewan, A.M., Yamaguchi, Y., Rahman, Z., 2012. Dynamics of land use/cover changes and the analysis of landscape fragmentation in Dhaka Metropolitan, 315–330. https://doi.org/10.1007/s10708-010-9399-x.

Downing, T., Olago, D., Nyumba, T., 2023. Perceptions of ecosystem services and climate change in the communities surrounding Mt. Kenya and Mt. Elgon, Kenya. Sustain. Times 15. https://doi.org/10.3390/su151411470.

Eckert, S., Kiteme, B., Njuguna, E., Zaehringer, J.G., 2017. Agricultural expansion and intensification in the foothills of Mount Kenya: a landscape perspective. Remote Sens. 9, 1–20. https://doi.org/10.3390/rs9080784.

Embu County Government, 2019. COUNTY INTEGRATED DEVELOPMENT PLAN 2018-2022.

Emerton, L., 1999. THE ECONOMICS OF COMMUNITY CONSERVATION.

FAO, 2020. Global forest resources assessment 2020: main report. Rome. https://doi.org/10.4324/9781315184487-1.

FAO, 2015. Global Forest Resources Assessment 2015, Rome, Italy.

Foley, J.A., Defries, R., Asner, G.P., Barford, C., Bonan, G., Carpenter, S.R., Chapin, F.S., Coe, M.T., Daily, G.C., Gibbs, H.K., Helkowski, J.H., Holloway, T., Howard, E.A., Kucharik, C.J., Monfreda, C., Patz, J.A., Prentice, I.C., Ramankutty, N., Snyder, P.K., 2005. Global consequences of land use. Science 5734, 570–575.

Fundi, P., 2020. Potential opportunities and threats to a reintroduced critically endangered mountain bongo population and its habitat at mount Kenya forest. Int. J. Nat. Resour. Ecol. Manag. 5, 102–107. https://doi.org/10.11648/j.ijnrem.20200503.13.

Gao, B.C., 1996. Ndwi - a normalized difference water index for remote sensing of vegetation liquid water from space. Remote Sens. Environ. 58, 257–266. https://doi.org/10.1016/S0034-4257(96)00067-3.

Geist, H.J., Lambin, E.F., 2002. Proximate causes and underlying driving forces of tropical deforestation. Bioscience 52, 143–150. https://doi.org/10.1641/0006-3568(2002)052[0143:PCAUDF]2.0.CO;2.

Gichuhi, M.W., Keriko, J.M., Mukundi, J.B.N., 2014. Ecosystem services to the community : a situation analysis of Mt . Kenya conservation area using GIS and remote sensing. Int. Conf. Sustain. Res. Innov. 5, 18–22.

Giriraj, A., Irfan-Ullah, M., Murthy, M.S.R., Beierkuhnlein, C., 2008. Modelling spatial and temporal forest cover change patterns (1973-2020): a case study from South Western Ghats (India). Sensors 8, 6132–6153. https://doi.org/10.3390/s8106132.

Goutte, C., Gaussier, E., 2005. A probabilistic interpretation of precision, recall and f-score. Eur. Conf. Inf. Retr 345–359.

Guo, J., Gong, P., Dronova, I., Zhu, Z., 2022. Forest cover change in China from 2000 to 2016 ABSTRACT. Int. J. Rem. Sens. 43, 593–606. https://doi.org/10.1080/01431161.2021.2022804.

He, C., Shi, P., Xie, D., Zhao, Y., 2010. Improving the normalized difference built-up index to map urban built-up areas using a semiautomatic segmentation approach. Remote Sens. Lett 1, 213–221. https://doi.org/10.1080/01431161.2010.481681.

Henry, M.C., Maingi, J.K., McCarty, J., 2019. Fire on the water towers: mapping burn scars on mount Kenya using satellite data to reconstruct recent fire history. Remote Sens. 11. https://doi.org/10.3390/rs11020104.

Hosonuma, N., Herold, M., De Sy, V., De Fries, R.S., Brockhaus, M., Verchot, L., Angelsen, A., Romijn, E., 2012. An assessment of deforestation and forest degradation drivers in developing countries. Environ. Res. Lett. 7. https://doi.org/10.1088/1748-9326/7/4/044009.

Hou, H., Zhou, B.B., Pei, F., Hu, G., Su, Z., Zeng, Y., Zhang, H., Gao, Y., Luo, M., Li, X., 2022. Future land use/land cover change has nontrivial and potentially dominant impact on global gross primary productivity. Earths Future 10, 1–20. https://doi.org/10.1029/2021EF002628.

Huang, S., Tang, L., Hupy, J.P., Wang, Y., Shao, G., 2021. A commentary review on the use of normalized difference vegetation index (NDVI) in the era of popular remote sensing. J. For. Res. 32, 1–6. https://doi.org/10.1007/s11676-020-01155-1.

Jebiwott, A., Ogendi, G.M., Agbeja, B.O., Alo, A.A., Kibet, R., 2021. Mapping the trends of forest cover change and associated drivers in Mau Forest, Kenya. Remote Sens. Appl. Soc. Environ. 23, 100586. https://doi.org/10.1016/j.rsase.2021.100586.

Jia, J., Hughes, A.C., Nunes, M.H., Santos, E.G., Pellikka, P.K.E., Kalliovirta, L., Mwangombe, J., Maeda, E.E., 2024. Forest structural and microclimatic patterns along an elevational gradient in Mount Kenya. Agric. For. Meteorol. 356, 110188. https://doi.org/10.1016/j.agrformet.2024.110188.

Jouzi, Z., Leung, Y.F., Nelson, S., 2022. Addressing the food security and conservation challenges: can be aligned instead of apposed? Front. Conserv. Sci. 3. https://doi.org/10.3389/fcosc.2022.921895.

Kamusoko, C., Wada, Y., Furuya, T., Tomimura, S., Nasu, M., Homsysavath, K., 2013. Simulating future forest cover changes in Pakxeng District, Lao People's Democratic Republic (PDR): implications for sustainable forest management. Land 2, 1–19. https://doi.org/10.3390/land2010001.

Karahalil, U., Zeki, E., Köse, S., 2009. The spatiotemporal forest cover changes in Köprülü Canyon National Park (1965 - 2008). Turkey 8, 4495–4507.

Kariuki, J., 2006. And Conservation Alternatives for Mount Kenya Common Heritage , Diverse Interests : Deforestation and Conservation Alternatives for Mount Kenya.

Kenya Forest Service, 2021. National Forest Resources Assesment Report 2021, Kenya.

Kenya Forest Service, 2015. Chuka Participatory Forest Management Plan 2015-2019.

Kenya Forest Service, 2010. Mt. Kenya Forest Reserve Management Plan 2010-2019, pp. 4–9.

Kenya National Bureau of Statistics, 2019. Kenya Population and Housing Census Volume 1: Population by County and Sub-county, Kenya. National Bureau of Statistics.

Kenya Wildlife Service, 2010. Mt Kenya Ecosystem Management Plan, pp. 2010–2020.

Kenya Wildlife Service, 1999. Aerial survey of the destruction of mt. Kenya. IMENTI AND NGARE NDARE FOREST RESERVES.

Kindu, M., Schneider, T., Döllerer, M., Teketay, D., Knoke, T., 2018. Scenario modelling of land use/land cover changes in Munessa-Shashemene landscape of the Ethiopian highlands. Sci. Total Environ. 622–623, 534–546. https://doi.org/10.1016/j.scitotenv.2017.11.338.

Kinoti, K., Mwende, K., 2019. Spatial-temporal assessment of forest rehabilitation along Mt. Kenya East forest buffer zone using remote sensing and GIS. Int. J. Environ. Plan. Dev. 5, 6–16.

Kinyili, B.M., 2023a. Leveraging on technologies in forest monitoring , surveillance and protection : the role of artificial intelligence (AI) in earth observation using time series. In: 12TH MARA DAY SCIENTIFIC CONFERENCE 14TH SEPTEMBER, 2023.

Kinyili, B.M., 2023b. Forest adjacent community perception on fencing for forest conservation around western Mt. Kenya forest. Int. J. For. Ecosyst. 1.

Kipkulei, H.K., Bellingrath-Kimura, S.D., Lana, M., Ghazaryan, G., Boitt, M., Sieber, S., 2022. Modelling cropland expansion and its drivers in trans nzoia county, Kenya. Model. Earth Syst. Environ. 8, 5761–5778. https://doi.org/10.1007/s40808-022-01475-7.

Kiria, E., Magana, A., Njue, C., 2019. Spatial-temporal changes in land use land cover and its impacts on wildlife conservation in Meru conservation area, Kenya. Asian J. Environ. Ecol. 1–10. https://doi.org/10.9734/ajee/2019/v10i330120.

Kogo, B.K., Kumar, L., Koech, R., 2021. Analysis of spatio-temporal dynamics of land use and cover changes in Western Kenya. Geocarto Int. 36, 376–391. https://doi.org/10.1080/10106049.2019.1608594.

Krieger, B.D.J., 2001. Economic Value of Forest Ecosystem Services : A Review.

Kumar, S., Radhakrishnan, N., Mathew, S., 2014. Land use change modelling using a Markov model and remote sensing. Geomatics Nat. Hazards Risk 5, 145–156. https://doi.org/10.1080/19475705.2013.795502.

Lambin, E.F., Coomes, O.T., Turner, B.L., Geist, H.J., Agbola, S.B., Angelsen, A., Folke, C., Bruce, J.W., Coomes, O.T., Dirzo, R., George, P.S., Homewood, K., Imbernon, J., Leemans, R., Li, X., Moran, E.F., Mortimore, M., Ramakrishnan, P.S., Richards, J.F., Vogel, C., Xu, J., 2001. The causes of land-use and land-cover change : moving beyond the myths. Glob. Environ. Change 11, 261–269.

Mahiga, S.N., Webala, P., Mware, M.J., Ndang'ang'a, P.K., 2019. Influence of land-use type on forest bird community composition in mount Kenya forest. Int. J. Ecol. 2019.

Maina, P.M., Nzengya, D.M., 2021. Trends in livestock grazing in the protected forests at mount Kenya region: evidence from year 2013 to 2018 using time series analysis. J. Pop. Educ. Africa 5, 38–52.

Margono, B.A., Potapov, P.V., Turubanova, S., Stolle, F., Hansen, M.C., 2014. Primary Forest Cover Loss in Indonesia over 2000–2012, vol. 4, pp. 730–735. https://doi.org/10.1038/NCLIMATE2277.

Mengist, W., Soromessa, T., Legese, G., 2021. Monitoring Afromontane forest cover loss and the associated socio-ecological drivers in Kaffa biosphere reserve , Ethiopia. Trees, For. People 6, 100161. https://doi.org/10.1016/j.tfp.2021.100161.

Ministry of Agriculture Livestock and Fisheries, 2017. Climate risk profile for Tharaka Nithi county. Kenya county climate risk profile series. Ministry of Agriculture Livestock and Fisheries (MoALF), Nairobi, Kenya.

Ministry of Environment and Natural Resources, 2016. Technical Report on the National Assessment of Forest and Landscape Restoration Opportunities in Kenya 2016 35.

Mishkin, M., Pacheco, N., 2022. Rapid Assessment Remote Sensing of Forest Cover Change to Inform Forest Management : Case of the Monarch Reserve, vol. 137. https://doi.org/10.1016/j.ecolind.2022.108729.

Muchena, F.N., Gachene, C.K.K., 1988. Soils of the highland and mountainous areas of Kenya with special emphasis on agricultural soils. Mt. Res. Dev. 8, 183–191.

Muhammad, R., Zhang, W., Abbas, Z., Guo, F., Gwiazdzinski, L., 2022. Spatiotemporal change analysis and prediction on future land use and land cover changes using QGIS MOLUSCE plugin and remote sensing big data: a case study of linyi, China. Land 11. https://doi.org/10.3390/land11030419.

Munsi, M., Areendran, G., Joshi, P.K., 2012. Modeling spatio-temporal change patterns of forest cover: a case study from the Himalayan foothills (India). Reg. Environ. Change 12, 619–632. https://doi.org/10.1007/s10113-011-0272-3.

Munthali, M.G., Mustak, S., Adeola, A., Botai, J., Singh, S.K., Davis, N., 2020. Modelling land use and land cover dynamics of Dedza district of Malawi using hybrid Cellular Automata and Markov model. Remote Sens. Appl. Soc. Environ. 17, 100276. https://doi.org/10.1016/j.rsase.2019.100276.

Muriithi, F.K., 2016. Land use and land cover (LULC) changes in semi-arid sub-watersheds of Laikipia and Athi River basins, Kenya, as influenced by expanding intensive commercial horticulture. Remote Sens. Appl. Soc. Environ. 3, 73–88. https://doi.org/10.1016/j.rsase.2016.01.002.

Mwabumba, M., Yadav, B.K., Rwiza, M.J., Larbi, I., Twisa, S., 2022. Analysis of land use and land-cover pattern to monitor dynamics of Ngorongoro world heritage site (Tanzania) using hybrid cellular automata-Markov model. Curr. Res. Environ. Sustain. 4, 100126. https://doi.org/10.1016/j.crsust.2022.100126.

Nature Kenya, 2019. Ecosystem service assessment for the restoration of mount Kenya forest. Nature Kenya, Nairobi.

Nayak, D., Shukla, A.K., Devi, N.R., 2024. Decadal changes in land use and land cover: impacts and their influence on urban ecosystem services. Aqua Water Infrastructure, Ecosyst. Soc. 73, 57–72. https://doi.org/10.2166/aqua.2024.211.

Notter, B., MacMillan, L., Viviroli, D., Weingartner, R., Liniger, H.P., 2007. Impacts of environmental change on water resources in the Mt. Kenya region. J. Hydrol. 343, 266–278. https://doi.org/10.1016/j.jhydrol.2007.06.022.

Nyongesa, K.W., Vacik, H., 2018. Fire Management in Mount Kenya: a case study of Gathiuru forest station. Forests 9. https://doi.org/10.3390/f9080481.

Pal, M., Maxwell, A.E., Warner, T.A., 2013. Kernel-based extreme learning machine for remote-sensing image classification. Remote Sens. Lett 4, 853–862. https://doi.org/10.1080/2150704X.2013.805279.

Paradis, E., 2021. Forest policy and economics forest gains and losses in Southeast asia over 27 years : the slow convergence towards reforestation. For. Policy Econ. 122, 102332. https://doi.org/10.1016/j.forpol.2020.102332.

Parracciani, C., Gigante, D., Mutanga, O., Bonafoni, S., Vizzari, M., 2024. Land cover changes in grassland landscapes: combining enhanced Landsat data composition, LandTrendr, and machine learning classification in google earth engine with MLP-ANN scenario forecasting. GIScience Remote Sens. 61. https://doi.org/10.1080/15481603.2024.2302221.

Pham-Duc, B., Nguyen, H., Phan, H., Tran-Anh, Q., 2023. Trends and applications of google earth engine in remote sensing and earth science research: a bibliometric analysis using scopus database. Earth Sci. Informatics 16, 2355–2371. https://doi.org/10.1007/s12145-023-01035-2.

Poletti, C., Dioszegi, G., Nyongesa, K.W., Vacik, H., Barbujani, M., Kigomo, J.N., 2019. Characterization of forest fires to support monitoring and management of mount Kenya forest. Mt. Res. Dev. 39, R1–R12. https://doi.org/10.1659/MRD-JOURNAL-D-18-00014.1.

Powers, D.M.W., 2020. Evaluation: from Precision, Recall and F-Measure to ROC, Informedness, Markedness and Correlation.

Reay, D., Sabine, C., Smith, P., Hymus, G., 2007. Intergovernmental Panel on Climate Change. Fourth Assessment Report. Geneva, Switzerland: Inter-gov- Ernmental Panel on Climate Change. Cambridge University Press Intergovernmental Panel on Climate Change, Cambridge; UK. https://doi.org/10.1038/446727a, 2007. www.ipcc.ch.

Reddy, C.S., Jha, C.S., Dadhwal, V.K., 2013. Assessment and monitoring of long-term forest cover changes in Odisha , India using remote sensing and GIS 4399–4415. https://doi.org/10.1007/s10661-012-2877-5.

Reddy, C.S., Singh, S., Dadhwal, V.K., Jha, C.S., Rao, N.R., Diwakar, P.G., 2017. Predictive modelling of the spatial pattern of past and future forest cover changes in India. J. Earth Syst. Sci. 126. https://doi.org/10.1007/s12040-016-0786-7.

Reed, J., Barlow, J., Carmenta, R., van Vianen, J., Sunderland, T., 2019. Engaging multiple stakeholders to reconcile climate, conservation and development objectives in tropical landscapes. Biol. Conserv. 238, 108229. https://doi.org/10.1016/j.biocon.2019.108229.

Rodriguez-Galiano, V.F., Ghimire, B., Rogan, J., Chica-Olmo, M., Rigol-Sanchez, J.P., 2012. An assessment of the effectiveness of a random forest classifier for land-cover classification. ISPRS J. Photogrammetry Remote Sens. 67, 93–104. https://doi.org/10.1016/j.isprsjprs.2011.11.002.

Rotich, B., Kindu, M., Kipkulei, H., Kibet, S., Ojwang, D., 2022. Impact of land use/land cover changes on ecosystem service values in the cherangany hills water tower, Kenya. Environ. Challenges 8, 100576. https://doi.org/10.2139/ssrn.4079129.

Rotich, B., Makindi, S., Esilaba, M., 2020. Communities attitudes and perceptions towards the status, use and management of Kapolet Forest Reserve in Kenya. Int. J. Biodivers. Conserv. 12, 363–374. https://doi.org/10.5897/ijbc2018.1448.

Rotich, B., Ojwang, D., 2021. Trends and drivers of forest cover change in the Cherangany hills forest ecosystem, western Kenya. Glob. Ecol. Conserv. 30, e01755. https://doi.org/10.1016/j.gecco.2021.e01755.

Rouse, J.W., Haas, R.H., Schell, J.A., Deering, D.W., 1974. Monitoring vegetation systems in the great plains with ERTS. Proceedings of the Third Earth Resources Technology Satellite-1 Symposium. NASA SP-351, Washington, D.C.

Rudel, T.K., Defries, R., Asner, G.P., Laurance, W.F., 2009. Changing drivers of deforestation and new opportunities for conservation. Conserv. Biol. 23, 1396–1405. https://doi.org/10.1111/j.1523-1739.2009.01332.x.

Sakieh, Y., Salmanmahiny, A., 2016. Performance assessment of geospatial simulation models of land-use change—a landscape metric-based approach. Environ. Monit. Assess. 188, 1–16. https://doi.org/10.1007/s10661-016-5179-5.

Sang, C.C., Olago, D.O., Ongeri, Z.J., 2023. The factors driving land cover transitions and land degradation and the potential impacts of the proposed developments in the Isiolo dam watershed, LAPSSET corridor, Kenya. Discov. Sustain 4. https://doi.org/10.1007/s43621-023-00126-w.

Saranya, K.R.L., Lakshmi, T.V., Reddy, C.S., 2022. Analysing the trends in annual forest loss hotspots in the regional landscape of Eastern Ghats , India. Remote Sens. Appl. Soc. Environ. 26, 100731. https://doi.org/10.1016/j.rsase.2022.100731.

Schmocker, J., Liniger, H.P., Ngeru, J.N., Brugnara, Y., Auchmann, R., Brönnimann, S., 2016. Trends in mean and extreme precipitation in the Mount Kenya region from observations and reanalyses. Int. J. Climatol. 36, 1500–1514. https://doi.org/10.1002/joc.4438.

Shravan Kumar, S.M., Pandey, M., Shukla, A.K., 2024. Spatio-temporal analysis of riverbank changes using remote sensing and geographic information system. Phys. Chem. Earth 136, 103692. https://doi.org/10.1016/j.pce.2024.103692.

Shukla, K.A., Shekhar Prasad Ojha, C., Mijic, A., Buytaert, W., Pathak, S., Dev Garg, R., Shukla, S., 2018. Population growth, land use and land cover transformations, and water quality nexus in the Upper Ganga River basin. Hydrol. Earth Syst. Sci. 22, 4745–4770. https://doi.org/10.5194/hess-22-4745-2018.

Simeon, M., Wana, D., 2024. Impacts of Land use Land cover dynamics on Ecosystem services in maze national park and its environs , southwestern Ethiopia. Heliyon 10, e30704. https://doi.org/10.1016/j.heliyon.2024.e30704.

Sitati, E.N., Abdallah, S., Olago, D., Marchant, R., 2024. Past and future land use and land cover trends across the mara landscape and the wider mau River basin, Kenya. Land 13, 1443.

Sokolova, M., Lapalme, G., 2009. A systematic analysis of performance measures for classification tasks. Inf. Process. Manag. 45, 427–437. https://doi.org/10.1016/j.ipm.2009.03.002.

Surya, B., Syafri, S., Sahban, H., Sakti, H.H., 2020. Natural resource conservation based on community economic empowerment: perspectives on watershed management and slum settlements in Makassar City, South Sulawesi, Indonesia. Land 9. https://doi.org/10.3390/land9040104.

Tadese, S., Soromessa, T., Bekele, T., 2021. Analysis of the current and future prediction of land use/land cover change UsingRemote sensingand the CA-MarkovModel in majang forest biosphere reserves of gambella, southwestern Ethiopia. Sci. World J. 2021.

Taloor, A.K., Singh Manhas, Drinder, Chandra Kothyari, G., 2021. Retrieval of land surface temperature, normalized difference moisture index, normalized difference water index of the Ravi basin using Landsat data. Appl. Comput. Geosci. 9, 100051. https://doi.org/10.1016/j.acags.2020.100051.

Tesfay, F., Tadesse, S.A., Getahun, Y.S., Lemma, E., 2023. Evaluating the impact of land use land cover changes on the values of ecosystem services in the Chacha Watershed , Ethiopia ' s central highland. Environ. Sustain. Indic. 18, 100256. https://doi.org/10.1016/j.indic.2023.100256.

The county government of Meru, 2018. Meru county integrated development plan. 2018-2022, Encyclopedia of Public Administration and Public Policy, second ed. (Print Version).

Thonfeld, F., Steinbach, S., Muro, J., Kirimi, F., 2020. Long-term land use/land cover change assessment of the Kilombero catchment in Tanzania using random forest classification and robust change vector analysis. Remote Sens. 12. https://doi.org/10.3390/rs12071057.

Tilahun, Z.A., Bizuneh, Y.K., Mekonnen, A.G., 2024. A spatio-temporal analysis of the magnitude and trend of land use/land cover changes in Gilgel Gibe Catchment, Southwest Ethiopia. Heliyon 10, e24416. https://doi.org/10.1016/j.heliyon.2024.e24416.

Townshend, J.R., Masek, J.G., Huang, C., Vermote, E.F., Gao, F., Channan, S., Sexton, J.O., Feng, M., Narasimhan, R., Kim, D., Song, K., Song, D., Song, X.P., Noojipady, P., Tan, B., Hansen, M.C., Li, M., Wolfe, R.E., 2012. Global characterization and monitoring of forest cover using Landsat data: opportunities and challenges. Int. J. Digit. Earth 5, 373–397. https://doi.org/10.1080/17538947.2012.713190.

Vanonckelen, Steven, Van Rompaey, A., 2015. Spatiotemporal analysis of the controlling factors of forest cover change in the Romanian carpathian mountains spatiotemporal analysis of the controlling factors of forest cover change in the Romanian carpathian mountains. Mt. Res. Dev. 35, 338–350.

Wahelo, T.T., Mengistu, D.A., Merawi, T.M., 2024. Spatiotemporal trends and drivers of forest cover change in Metekel Zone forest areas, Northwest Ethiopia. Environ. Monit. Assess. 196, 1170. https://doi.org/10.1007/s10661-024-13294-7.

Wiesmann, U., Gichuki, F.N., Kiteme, B.P., Liniger, H., 2000. Mitigating conflicts over scarce water resources in the highland-lowland system of Mount Kenya. Mt. Res. Dev. 20, 10–15. https://doi.org/10.1659/0276-4741(2000)020[0010:MCOSWR]2.0.CO;2.

Winkler, K., Fuchs, R., Rounsevell, M., Herold, M., 2021. Global land use changes are four times greater than previously estimated. Nat. Commun. 12, 1–10. https://doi.org/10.1038/s41467-021-22702-2.

Yahya, N., Bekele, T., Gardi, O., Blaser, J., 2020. Forest cover dynamics and its drivers of the Arba Gugu forest in the Eastern highlands of Ethiopia during 1986 – 2015. Remote Sens. Appl. Soc. Environ. 20, 100378. https://doi.org/10.1016/j.rsase.2020.100378.

Yue, W., Qin, C., Su, M., Teng, Y., Xu, C., 2024. Environmental and Sustainability Indicators Simulation and prediction of land use change in Dongguan of China based on ANN cellular automata - Markov chain model. Environ. Sustain. Indic. 22, 100355. https://doi.org/10.1016/j.indic.2024.100355.

Zaehringer, J.G., Wambugu, G., Kiteme, B., Eckert, S., 2018. How do large-scale agricultural investments affect land use and the environment on the western slopes of Mount Kenya? Empirical evidence based on small-scale farmers' perceptions and remote sensing. J. Environ. Manag. 213, 79–89. https://doi.org/10.1016/j.jenvman.2018.02.019.

Zha, Y., Gao, J., Ni, S., 2003. Use of normalized difference built-up index in automatically mapping urban areas from TM imagery. Int. J. Rem. Sens. 24, 583–594. https://doi.org/10.1080/01431160304987.